



AUT
UNIVERSITY

NEW ZEALAND

Quantification of Sterol Glucosides in Tallow-Derived-Biodiesel by Liquid Chromatography with Tandem Mass Spectrometry

Kalita Theresa Clark Tongotea

A thesis submitted to
Auckland University of Technology
In partial fulfilment of the requirements for the degree of Master of Applied Science (MAppSc)

May 2018

School of Applied Science
Primary Supervisor: Dr. Chris Pook
Secondary Supervisor: Mark Duxbury

Declaration

"I hereby declare that this submission is my own work and that, to the best of my knowledge and belief, it contains no material previously published or written by another person (except where explicitly defined in the acknowledgements), nor material which to a substantial extent has been submitted for the award of any other degree or diploma of a university or other institution of higher learning."

Date: 18-05-2018

Abstract

Biodiesel is an important low-carbon substitute for petroleum diesel that behaves similarly in combustion engines to petroleum diesel. It has the advantages of being sourced from a wide range of renewable feedstocks, domestic origin, cleaner emission, non-toxicity, and superior lubricating properties. Unfortunately, engine problems related to degradation and deposit formation have resulted from the use of this renewable fuel. These issues are associated with the presence of plant-derived compounds called sterol glucosides [SGs], a sterol is bound to a glucopyranose through an O-ether bond, and their acylated analogues [ASGs]. During the transesterification reaction that produces biodiesel the acyl chain is often liberated from the ASG, yielding an increased concentration of SGs in the product. Under certain conditions SGs can precipitate as a white solid in the biodiesel fuel which can accumulate in filters and critical pipelines in the engines preventing the flow of fuel. Monitoring the levels of these compounds is critical as they directly affect the quality and development of biodiesel. Current analytical techniques for SGs and ASGs in feedstock and biodiesel product involve either gas-liquid chromatography [GC] or High-Pressure Liquid Chromatography [HPLC]. Neither method is straightforward as SGs and ASGs are not volatile and so require derivatisation for GC analysis. They do not absorb light strongly nor exhibit fluorescence and so HPLC detection must be by less sensitive techniques, such as Evaporative Light Scattering. These analyses are also complicated by the complex matrix of the feedstock and biodiesel product and are generally not specific to individual SGs but provide collective quantification. The objective of the present study was to develop an analytical method for the three most commonly reported plant-derived SGs in biodiesel using Liquid Chromatography with Tandem Mass Spectrometry [LC-MS/MS] that is simple, sensitive and specific. The final method involves saponification of the biodiesel, followed by extraction of the SGs to remove matrix effects and their acetylation to yield target compounds that are amenable to LC-MS/MS. A concentration step was necessary to yield highly sensitive results, providing a Method Detection Limit of 10.1 mg L^{-1} for each SG in biodiesel. This final method was highly specific to the three target compounds although due to the multiple extraction, derivatisation and concentration steps it cannot be claimed to achieve the desired goal of simplicity.

Acknowledgements

My Masters has been an inspiring and challenging project, which would not have been possible without the support and encouragement from my supervisor, Dr Chris Pook. Dude! It has been such an honour and a blessing to have been able to learn from you. You have inspired me to achieve at levels higher than I thought were even possible. Thank you for allowing me the opportunity to pursue my dreams and ambitions. Your guidance and assistance has enabled me to achieve my masters and also help me to grow as a scientist. Thank you for everything you have done, and most importantly for imparting your knowledge and expertise on the LC-MS/MS.

I would also like to express my appreciation and gratitude to Mark Duxbury, thank you for the valuable discussion and suggestions that helped complete this thesis.

I sincerely want to thank everyone at Independent Petroleum Laboratory, thank you for your encouragement and allowing me the time and resources to complete this thesis.

Finally, I would like to thank my family and in particular my fiancé. With your consent love and support, I have been able to pursue my passion and complete my studies, I can't thank you enough my love.

Above all, to God Almighty, thank you for your unconditional love.

Contents

Declaration	1
Abstract	2
Acknowledgments	3
Contents	4
List of Abbreviations	6
List of Figures	7
List of Tables	10
Introduction	11
Chapter 1 – Literature review	12
1.1 Biodiesel Background	12
1.2 Biodiesel Composition	13
1.3 Advantages and Disadvantages of Biodiesel	14
1.4 Properties and Specification of Biodiesel	16
1.5 Chromatographic Techniques	18
1.5.1 Brief Introduction to Mass Spectrometry	19
1.5.2 Ionisation techniques	19
1.5.3 Tandem Mass Spectrometry	22
1.5.4 Sterol Glucosides	23
1.5.5 Techniques for Sterol Glucoside Analysis	24
Thesis Objectives	27
Chapter 2 – Analysis of native sterol glucoside by LC-MS	28
2.1 Introduction	28
2.2 Experimental	29
2.3 Results	34
2.4 Discussion	42

Chapter 3 – Analysis of sterol glucoside by silylation and GC-MS	45
3.1 Introduction	45
3.2 Experimental	46
3.3 Results	47
3.4 Discussion	53
Chapter 4 – Acetylation of the sterol glucoside and quantification by LC-MS/MS	54
4.1 Introduction	54
4.2 Experimental	55
4.3 Results	59
4.4 Discussion	67
Chapter 5 – Trace Analysis of SGs in plant-based biodiesel	69
5.1 Introduction	69
5.2 Experimental	70
5.3 Results	73
5.4 Discussion	76
Chapter 6 – Summary and Recommendation	78
References	79

List of Abbreviations

ASTM	American Society for Testing and Materials
EN	European Standards
BX	Biodiesel blend with petro-diesel, where X is the percentage of biodiesel added
SGs	Sterol glucosides
ASGs	Acyl sterol glucoside
TGs	Triacylglycerides
HC	Hydrocarbon
PM	Particulate matter
SOx	Oxides of sulphur including Sulphur dioxide
SO ₃	Sulphur dioxide
CO	Carbon monoxide
NOx	Oxides with nitrogen group
LC	Liquid chromatography
GC	Gas chromatography
m/z	Mass-to-charge ratio
ESI	Electrospray Ionisation
EI	Electron Impact
CI	Chemical ionisation
MALDI	Matrix-assisted laser Desorption/Ionisation
APPI	Atmospheric Pressure Photoionization
APCI	Atmospheric Pressure Chemical Ionisation
ESI	Electrospray Ionisation
HPLC	High-Pressure Liquid chromatography
TOF	Time-of-Flight
QQQ	Triple Quadrupole
MS	Mass Spectrometry
PIS	Product Ion Scan
NL	Neutral Loss Scan
SIM	Selective Ion Monitoring Scan
MRM	Multiple Reaction Monitoring Scan
CID	Collision-Induced Dissociation
SiGluc	Sitosterol Glucoside
CaGluc	Campesterol Glucoside
StGluc	Stigmasterol Glucoside
NMR	Nuclear Magnetic Resonance
HMS	High-Resolution Mass Spectrometer
QTOF	Quadrupole-Time-of-Flight

List of Figures

Figure 1. Structural illustration of acylated campesterol glucoside (right), a red circle highlights the ester bond between the fatty acid chain and the glucose molecule. Campesterol glucoside (left) (Songtawee, et al., 2014)	11
Figure 2. A simple equation illustrating the reaction that occurs in transesterification (Leung, et al., 2010).....	13
Figure 3. Illustrates the emission of air pollutants from different blends of Soy-based biodiesel in 2010. The monitored pollutants include nitrogen oxide [NO _x], carbon monoxide [CO], hydrocarbons [HC], and Particulate matter [MP]. This graph was obtained from Teixeira, et al., 2012.	15
Figure 4. Liquid chromatography combined with tandem mass spectrometer	18
Figure 5. Illustration of a typical mass spectrometer outlining the three main components.	19
Figure 6. Illustration of ESI producing protonated ions (Banerjee & Mazumdar, 2012)	20
Figure 7 . A schematic diagram of an APCI ionisation source	21
Figure 8. A simple illustration of the different scan modes used in tandem quadrupole. For this study, Collision-Induced Dissociation [CID] was used to fragment the ions in the second quadrupole.....	23
Figure 9. Chemical structure of campesterol glucoside (A), stigmasterol glucoside (B), and sitosterol glucoside (C).	24
Figure 10. HPLC chromatogram of biodiesel, highlighting the peak for sterol glucoside (Wang, et al., 2009)....	25
Figure 11. Tallow based biodiesel, obtained from Independent Petroleum Laboratory [IPL].	30
Figure 12. A heat map of the SGs present in Lecithin. This shows the acetic adducts [M + HAC – H] ⁻ , which are labelled with numbers. And the chlorine adducts [M + Cl] ⁻ are labelled alphabetically, can also be seen to align with the acetic adducts with a difference of m/z 24, as seen in the table below.....	36
Figure 13. Heatmap of the total ion count for lecithin in negative mode. The scan ranged from 850 to 910 m/z, as described in the experimental section of Method B. The acetic adducts of the ASGs [M + HAC – H] ⁻ are highlighted and assigned numbers, as listed in the table below.	37
Figure 14. An identical heatmap from Figure 13. This illustrates the chlorine adducts that align with the acetic adduct of the ASGs, with a difference of 24 m/z. From this heat map we can identify the chlorine adduct for the acyl SiGluc.	38
Figure 15. Reconstructed negative ion chromatogram after LC-MS/MS analysis with MS1 set to scanning mode. The mass spectrum for the following SG species are shown with both acetic and chlorine adducts; (A) cholesterol glucoside, (B) campesterol glucoside, (C) stigmasterol glucoside, and (D) sitosterol glucoside.	39
Figure 16. Standard curve of cholesterol glucoside. A linear behaviour can be observed with y=212.15x, and a correlation coefficient r ² = 0.996.....	41

Figure 17. A comparison of the total-ion chromatogram of the blank (A), cholesterol glucoside(B), and glucose (C), after BSTFA derivatization. The inset shows a small peak present in only the cholesterol glucoside scan at 1995 seconds.	48
Figure 18. Mass spectrum and structure of penta(trimethyl)silylated [TMSi]-glucose. The spectrum was extracted from the TIC of glucose seen in Figure 17, which had a scan range of 48 to 800 m/z. Several high mass ions in the spectrum are formed by the loss of neutral fragments, typical of TMS derivatives. m/z 73, $(\text{CH}_3)_3\text{Si}^+$; m/z 117, $(\text{CH}_3)_3\text{SiOCH}_2\text{CH}_2^+$; m/z 147, $[(\text{CH}_3)_3\text{Si}^+]_2$; m/z 204, $[(\text{CH}_3)_3\text{Si}^+]_3$; lastly, m/z 305 $[(\text{CH}_3)_3\text{Si}]_4\text{CH}_2^+$. Although the molecular ion of 540 m/z was not observed.	49
Figure 19. Mass spectrum and structure of tetra(trimethyl)silylated [TMSi] cholesterol glucoside. Characteristic ions of TMSi-glucose can be seen the mass spectrum, as described in Fig 18.	50
Figure 20. EIC of the 73 m/z, 147 m/z, and 204 m/z with their corresponding blanks as the top chromatogram. The retention time for each characteristic ion of TMSi-glucose all elute out in the same time window with the two distinct peaks seen in the TIC of glucose in figure 17 at 570 and 590 seconds.	51
Figure 21. EIC of characteristic fragments of m/z 73, 147, 204, 217 from figure 17, at 2000 seconds.	52
Figure 22. The acetylation reaction of campesterol glucoside with acetic anhydride.	54
Figure 23. Image of the biodiesel sample, analysed in this chapter. All were acquired from IPL.	55
Figure 24. Derivatisation scheme for the reaction between campesterol glucoside and acetic anhydride in the presences of imidazole at room temperature	59
Figure 25. Mass spectra of each acetylated SG peak obtained from LC-MS of native sterol glucosides standards. (A) Cholesterol glucoside; (B) Stigmasterol glucoside; (C) Campesterol glucoside; (D) Sitosterol glucoside.	60
Figure 26. Extracted Ion Chromatograms illustrating complete acetylation of cholesterol glucoside. (A) m/z 608.5 corresponding to acetylation of one hydroxyl group; (B) m/z 650.5 for two hydroxyls; (C) m/z 692.5 for three acetylated hydroxyls; Lastly, (D) m/z 734.5 for all four hydroxyl groups being acetylated.....	61
Figure 27. Product ion scans of the acetylated SGs, obtained using CID with collision energy at 15 V and fragmentor voltage at 135 V. (A) cholesterol glucoside, m/z 734.5; (B) campesterol glucoside, m/z 748.5; (C) stigmasterol glucoside, m/z 760.5; (D) sitosterol glucoside, m/z 762.5.	63
Figure 28. TIC chromatogram from LC-MS/MS of acetylated (A) cholesterol glucoside, (B) mix sterol glucoside standard, (C) Lecithin.	64
Figure 29. Standard curve for cholesterol glucoside tetraacetate. The concentration ranged from 250 to 0.488 mg/L, with an excellent linear regression, $r^2 > 0.999$ and $y = 7.008x$	65
Figure 30. MRM chromatograms for cholesterol glucoside tetraacetate in a blank (A), lecithin (B) and two biodiesel samples (C) & (D). A 50 μL volume of 500 mg/L cholesterol glucoside was spiked into each sample prior to acetylation.	66

Figure 31. Plant based biodiesel acquired from Independent Petroleum Laboratory [IPL]. 70

Figure 32. Effect of different masses of biodiesel upon peak area of the internal standard. 73

Figure 33. Calibration curve of cholesterol glucoside tetraacetate with a range of 62.5 mg/L to 0.488 mg/L.
With a liner relationship, $y = 43.50x$, and $r^2 = 0.9997$ 75

List of Tables

Table 1. Table of the different oils species that can be used for biodiesel production (Leung, et al., 2010) ...	14
Table 2. Biodiesel specification for vehicle use according to American Standard (ASTM D-6751) and European Standard (EN 14214) (Reddy, 2017).....	166
Table 3. Gradient elution used to Separate the ASG by liquid chromatography.....	32
Table 4. Elution gradient used for the separation of SGs by LC-MS	32
Table 5: Parameters used for Selective Ion Monitoring of sterol glucosides	33
Table 6. Identification of the acetic and chlorine adducts for the SGs	36
Table 7. Characterisation of the acetic adducts of the ASGs	37
Table 8. Characterisation of the chlorine adducts of the ASGs	38
Table 9. Profile of sterol glucoside and acyl sterol glucoside	40
Table 10. Separation condition used in Method B.....	43
Table 11. Method A LC-MS conditions for full scan of acetylated SGs	577
Table 12. Method B is LC-MS/MS conditions for MRM analysis of acetylated SGs.....	588
Table 13. Formula and calculated m/z of cations for tetraacetylated derivatives of glucose and four sterol glucosides.	59
Table 14. MS/MS parameters for multiple ion monitoring [MRM] for the investigated sterol glucoside derivatives in the positive ESI.....	62
Table 15. Method A LC-MS conditions in Negative mode.	71
Table 16. Method B LC-MS/MS conditions for ESI-MRM scan in positive mode.	72
Table 17. The investigation of Matrix Effect by response factor, and comparison of solvent extraction.	744
Table 18. The concentration of SGs measured in biodiesel.....	755
Table 19. Summary of the limits of method presented in this thesis	777

Introduction

In recent decades, the decline of petroleum resources and improved awareness of climate change has intensified the search for alternative fuels that are renewable, sustainable, economically competitive, and have more environmental benefits (Demirbas., 2008; Owusu & Asumadu-Sarkodiw., 2016). Biodiesel is a popular candidate set to replace a significant percentage of petroleum diesel. Biodiesel fuel is a mixture of mono alkyl esters of long fatty acid chains, a product produced from a catalysed reaction between a low molecular weight alcohol such as methanol and triacylglycerides found in fats and oil. This renewable fuel must meet the specified ASTM and EN standards. Biodiesel behaves similarly in combustion engines to petroleum diesel, with the added advantage of a wide range of potential renewable feedstock, domestic origin, cleaner emission, non-toxicity, and superior lubricating properties (Hassan & Abul Kalam, 2013). An added advantage is that biodiesel can be blended with any portion of petroleum diesel, reducing toxic emissions. These fuels are referred to as BX, where X is the percentage of blended biodiesel; for example, a 20 percent blend of a pure biodiesel [B100] is referred to as B20. Unfortunately, there have been several engine problems related to degradation and deposit formation linked to the use of this renewable fuel (Hassan & Abul Kalam., 2013; Zuleta, et al., 2012). These problems have been connected to the presence of contaminants in biodiesel called sterol glucosides (Bondioli, et al., 2008; Hoed, et al., 2008; Pfalzgraf, et al. 2007).

Sterol glucosides [SGs] are comprised of a sterol bound to a glucopyranose through an O-ether bond. They are naturally abundant in plant tissue, as Acylated Sterol Glucosides [ASGs] which have a long fatty acid chain esterified to carbon six of the sugar moiety, as seen in Figure 1. During the catalyzed reaction, the fatty acid chain is broken off from the glucose molecule to form SGs, which have significantly lower solubility in biodiesel than ASGs and a high melting point. Under certain conditions SGs can precipitate as a white solid in the biodiesel fuel which can accumulate in filters and critical pipelines in the engines, preventing the flow of fuel (Bondioli, et al., 2008). Monitoring the levels of these compounds is critical as they directly affect the quality and development of biodiesel.

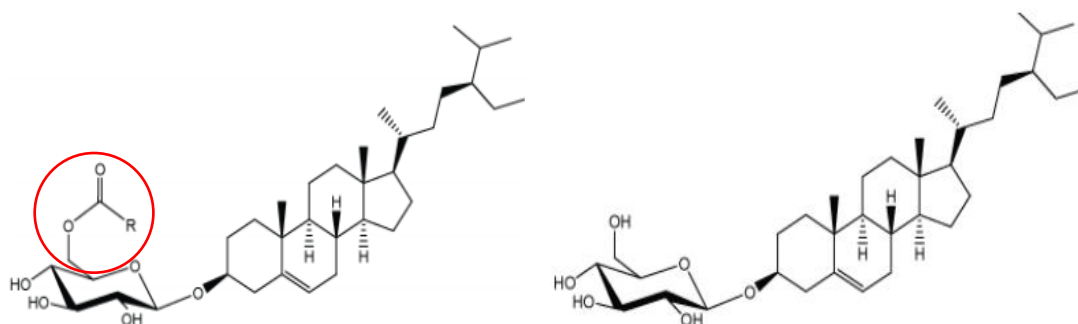


Figure 1. Structural illustration of acylated campesterol glucoside (right), a red circle highlights the ester bond between the fatty acid chain and the glucose molecule. Campesterol glucoside (left) (Songtawee, et al., 2014)

Chapter 1. Literature Review

This section will focus on the chemistry of sterol glucosides [SGs] and the possible reaction they undergo which can affect and alter their compositions in biodiesel. I will also discuss the parameters that define the quality of biodiesel. A brief overview on mass spectrometry will also be included. Lastly, I will evaluate analytical methods that have been used to quantify the concentration of SGs. The manufacturing process of biodiesel is out of the scope of this work and will be mentioned in certain sections but not expanded on.

1.1 Biodiesel Background

In 1895, German inventor Rudolph Diesel was granted the patent for his design of an internal combustion engine, commonly known as the diesel engine (Diesel, 1895). Surprisingly, Rudolph Diesel had designed the engine to run on vegetable oil with the aim of allowing farmers to produce their own fuel to run their diesel engines (Guo, et al., 2015). In the 1900s, he successfully demonstrated that the diesel engine can function when fuelled by peanut oil at the World Exhibition in Paris (Guo, et al., 2014; Stauffer & Byron, 2007). In fact, Rudolph Diesel stated (Borgman, 2007): “The use of vegetable oils for engine fuels may seem insignificant today, but such oils may become - in the course of time - as important as petroleum and coal-tar products of the present time.” Despite this prediction made over a century ago, discoveries of large petroleum reservoirs in the 1940s quickly muted the development of vegetable oil as a viable fuel (Guo, et al., 2015). Research on vegetable oils continued, although it soon became apparent that their viscosity made their use in diesel engines difficult. In the 1930’s Belgian scientist George Chavanne discovered that transesterification of raw vegetable oils, yielded functional biodiesel (Guo, et al., 2014; Knothe, 2001).

Biodiesel, defined as mono-alkyl esters of fatty acid chains, is used as an alternative or a partial substitute to petroleum diesel, referred to as mineral diesel or petro-diesel (Mateparae, 2011). Typically, biodiesel is refined from renewable feedstock like vegetable oil or animal fats through the process of transesterification. This is when the triacylglycerides in the oils or fats are mixed with an alcohol, usually methanol, to produce mono-alkyl ester and glycerol (Guo, et al., 2015). Although biodiesel has been highly researched, there are still considerable challenges associated with the quality of the final product including the different blends of biodiesel with mineral diesel. This is because the initial techniques used to analyse biodiesel were originally designed separately for oils and petroleum products (Eide & Zahlse, 2007).

1.2 Biodiesel Composition

The feedstock used to produce biodiesel are highly diverse and rich with triacylglycerides, as seen in Table 1. Although this is fairly significant, the selection of feedstocks is often determined by the availability of land and resources, economics, cultivation requirements, and oil composition (Gui, et al., 2008). As can be seen, each source varies in composition of fatty acids. This is illustrated through the different carbon numbers and degree of saturation. The oil composition can affect the properties of the final product of biodiesel such as viscosity, rate of combustion, cetane number and melting points (Leung, et al., 2010; Pinto, et al., 2005). The selection of feedstock is crucial as it accounts for nearly 60-80% of production cost (Leung, et al., 2010).

Triacylglycerides [TGs] are esters that contain three fatty acids and a glycerol molecule, as seen below in Figure 2. As mentioned previously, biodiesel is produced through transesterification. Chemically, transesterification means the ester bonds between the fatty acid and glycerol are broken which allows the alcohol group to react with fatty acid to produce three fatty-acid-alcohol-esters and glycerol. Generally, this is a slow reaction and often requires the aid of a catalyst (Leung, et al., 2010; Fukuda, et al., 2001). Once complete reaction is achieved, two distinct phases of glycerol and biodiesel are formed. Biodiesel is then required to further undergo several pre-treatments to remove any trace of catalyst, alcohol, glycerol, and other contaminants.

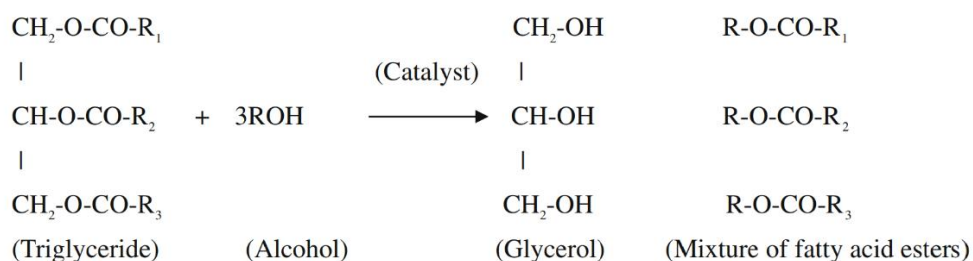


Figure 2. A simple equation illustrating the reaction that occurs in transesterification (Leung, et al., 2010)

Table 1. Table of the different oils that can be used for biodiesel production (Leung, et al., 2010)

Types of oils	Species	Main fatty acid composition
Edible oils	Soybean	C16:0, C18:1, C18:2
	Sunflower	C16:0, C18:0, C18:1, C18:2
	Palm	C16:0, C18:0, C18:1, C18:2
	Peanut	C16:0, C18:0, C18:1, C18:2, C20:0, C22:0
	Corn	C16:0, C18:0, C18:1, C18:2, C18:3
	Camelina	C16:0, C18:0, C18:1, C18:2, C18:3, C20:0, C20:1, C20:3
	Canola	C16:0, C18:0, C18:1, C18:2, C18:3
	Cotton	C16:0, C18:0, C18:1, C18:2
	Pumpkin	C16:0, C18:0, C18:1, C18:2
	Jatropha curcas	C16:0, C16:1, C18:0, C18:1, C18:2
	Non-edible oil	Pongamina pinnata
Sea mango		C16:0, C18:0, C18:1, C18:2
Palanga		C16:0, C18:0, C18:1, C18:2
Tallow		C14:0, C16:0, C16:1, C17:0, C18:0, C18:1, C18:2
Nile tilapia		C16:0, C18:1, C20:5, C22:6, other acids
Poultry		C16:0, C16:1, C18:0, C18:1, C18:2, C18:3
OTHERS		Used cooking oil

1.3 Advantages and Disadvantages of Biodiesel

Biodiesel possesses several advantages over petro-diesel. Environmentally, biodiesel as a net or blended fuel, can drastically reduce the emission of air pollutants such as hydrocarbon [HC], particulate matter [PM], sulphur oxides [SOx] and carbon monoxide [CO] (Frey & Kim, 2005; Teixeira, et al., 2012). Figure 3 illustrates the emission of air pollutants by biodiesel in different concentrations. Unfortunately, the levels of nitrogen oxide [NOx] is greater than mineral diesel which contributes to the formation of smog and acid rain, consequently harming both environmental and human health (Teixeira, et al., 2012; Air Quality Expert Group, 2004). It is important to remember that the emission of these pollutants depends on the type of feedstock and engine design, as they both can affect the fuel's combustion rate. In terms of safety, the risks associated with handling, transporting and storing biodiesel are seen to be lower than petro-diesel because it has a higher flash point and decomposes at a faster rate than petro-diesel (Demirbas, 2009; Hassan & Abul Kalam, 2013; Leung, et al., 2010). This makes biodiesel more appealing, especially when oil spills have occurred more frequently in the past decade and threaten the health of important habitats. Politically,

domestic production of biodiesel reduces dependency on imported fuels. It also enhances energy security and encourages growth in the agricultural sector (Tomei & Helliwell, 2016). However, concerns around the use of valuable crop-land could affect the cost of food, which can lead to food scarcity (Tenenbaum, 2008). An alternative is to use inedible sources like tallow and waste oils. Economically, the design of the diesel engine will require little or no modification with the added advantage of reducing wear and tear of the engines, because biodiesel has superior lubricity over petro-diesel (Agarwal, et al., 2011).

One of the main disadvantages of biodiesel, is that commercialization is hindered by the high cost of production. Because of this, producers rely heavily on government support through the provision of tax incentives and subsidy schemes to allow biodiesel to match the market value with fossil fuels (Josling, et al., 2010; Koplow, et al., 2006; Kutas, et al., 2007; Lopez & Laan, 2008). Although the New Zealand government had allocated \$36 million to the biofuel industry between 2009 and 2012, Z Energy set out to produce biodiesel derived from tallow without any support from the government. Initial production cost was estimated around \$26 million dollars, with a goal of producing 20 million litres of biodiesel per year (Bradley, 2014). Lastly, engine failure has been linked to minor compounds present in biodiesel such as sterol glucoside [SGs]. These contaminants affect the cold flow property and decrease the quality of biodiesel (Bondioli, et al., 2008; Hoed, et al., 2008; Lee, et al., 2007; Monirul, et al., 2015; Pfalzgraf, et al. 2007).

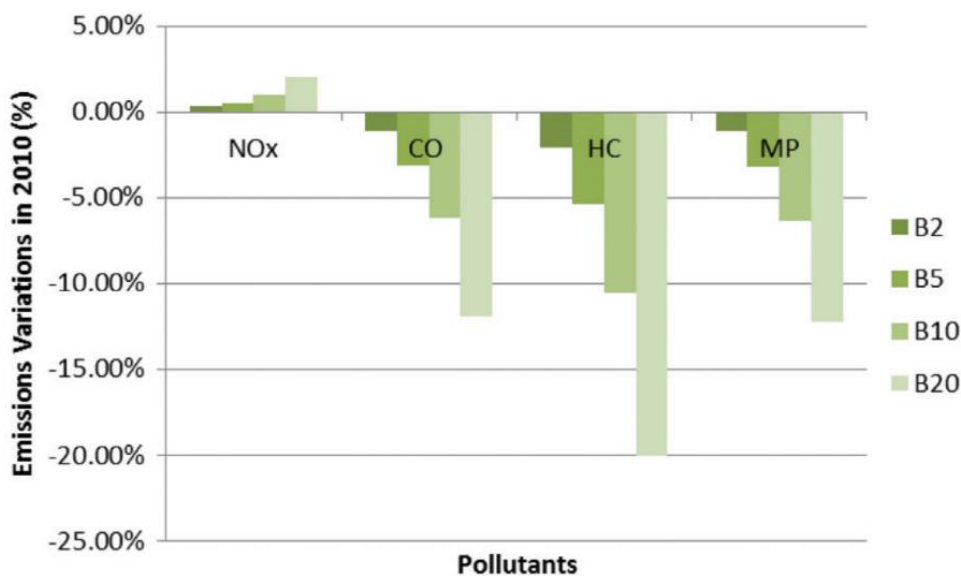


Figure 3. Illustrates the emission of air pollutants from different blends of Soy-based biodiesel in 2010. The monitored pollutants include nitrogen oxide [NO_x], carbon monoxide [CO], hydrocarbons [HC], and Particulate matter [MP]. This graph was obtained from Teixeria, et al., 2012.

1.4 Properties and Specification of Biodiesel

The quality of biodiesel is critical for performance and acceptance into the market as a valuable commodity. Globally, standard specifications are set to measure the quality and risk associated with fuel, to ensure a level of confidence and security for all parties involved, such as manufactures, producers and consumers. The two most common standards used for biodiesel can be seen in Table 2. These are the American Society for Testing and Materials ASTM D6751, and European Standard EN14214. As seen in Table 2, several methods are used to measure both the physical and chemical properties of biodiesel such as density, viscosity, flash point, acid value, and methyl ester contents. The final product must meet the specified standards. In some cases, the specifications used for petro-diesel have been transferred to biodiesel, but due to the differences in properties between the fuels, not all specification of diesel are suitable for biodiesel (Knothe, 2001; Yasin, et al., 2013). As stated previously, the presence of SGs in biodiesel affects the performance and quality of the fuel. Currently there are no standards set to monitor and define the limits of SGs in biodiesel. Consequently, they fall under the umbrella of EN 12662 for total contamination. As seen in Table 2, if the concentration of total contaminates exceed the limit of 24 mg/kg according to the EN 12662 method, this renders the fuel outside the specification limits of EN 14214:2017, and cannot be sold as a viable fuel. Evidence has shown that the filterability of the fuel is still affected when SGs are present at 10 mg/kg (Pfalzgraf, et al., 2007). Therefore, it is important to develop a method for detecting low levels of SGs in biodiesel, which will allow producers to monitor the presence of SGs before, during, and after production.

Table 2. Biodiesel specification for vehicle use according to American Standard (ASTM D-6751) and European Standard (EN 14214) (Reddy, 2017)

Properties	Units	Limits	Test method
Fatty acid methyl esters	% mass	96.5 min	EN 14103
Density at 15°C	kg/m ³	860 min 900 max	ASTM D1298 or ASTM D4052
Viscosity at 40°C	mm ² /s	2.0 min 5.0 max	ASTM D445
Flash point	°C	100 min	ASTM D93
Sulphur	mg/kg	10 max	IP 497 or ASTM D5453
Carbon residue (on 100% distillation residue)	% mass	0.05 max	ASTM D4530
Cetane number		51 min	ASTM D613 or ASTM D6890

Table 2. Continued

Properties	Units	Limits	Test method
Sulphated ash content	% mass	0.020 max	ASTM D874
Water	mg/kg	500 max	IP 438
Total contamination	mg/kg	24 max	EN 12662
Copper strip corrosion (3 hours at 50°C)		Class 1 max	ASTM D130
Oxidation stability, 110°C	hours	8.0 min	EN 14112 or EN 15751
Acid value	mg KOH/g	0.50 max	ASTM D664
Iodine value	g iodine/100 g	140 max	EN 14111
Linolenic acid methyl ester	% mass	12.0 max	EN 14103
Polyunsaturated (≥ 4 double bonds) methyl esters	% mass	1 max	EN 15779
Methanol	% mass	0.20 max	EN 14110
Monoacylglycerides	% mass	0.80 max	ASTM D6584
Diacylglycerides	% mass	0.20 max	ASTM D6584
Triacylglycerides	% mass	0.20 max	ASTM D6584
Free glycerol	% mass	0.020 max	ASTM D6584
Total glycerol	% mass	0.25 max	ASTM D6584
Group I metals (Na+K)	mg/kg	5.0 max	EN 14538 or EN 14108 and EN 14109
Group II metals (Ca+Mg)	mg/kg	5.0 max	EN 14538
Phosphorus	mg/kg	4.0 max	EN 14107 and EN 16294

1.5 Chromatography

Chromatography is an analytical technique widely used for the identification and purification of compounds in a mixture (Coskun, 2016; Yahaya, et al., 2013). Essentially it is the study of how the compounds can be separated by their fundamental properties. Generally, a gas or liquid medium termed the 'mobile phase' flows through a solid medium referred to as stationary phase. The stationary phase can either be a solid absorbent or a liquid that is coated on an inert support like glass beads or fused silica (Coskun, 2016; Rahman, et al., 2015). Target compounds are carried by mobile phase and the separation is determined by how they interact with the stationary phase to slow or arrest their movement. There are different chromatography techniques available such as, ion-exchange chromatography, thin-layer chromatography, gas chromatography [GC], and liquid chromatography [LC], which all employ these same basic principles. In this study GC and LC are the two chromatographic techniques used to analyse the SGs. In GC the mobile phase is an inert gas usually helium or nitrogen, and often requires the samples to be in a gaseous phase. While LC uses a liquid mobile phase and is commonly used for any sample that can be solubilised in a liquid. Both the LC and GC can be combined to a wide range of detectors including mass spectrometry. Below in Figure 4, is the LC system combined with a tandem mass spectrometer used in this study.

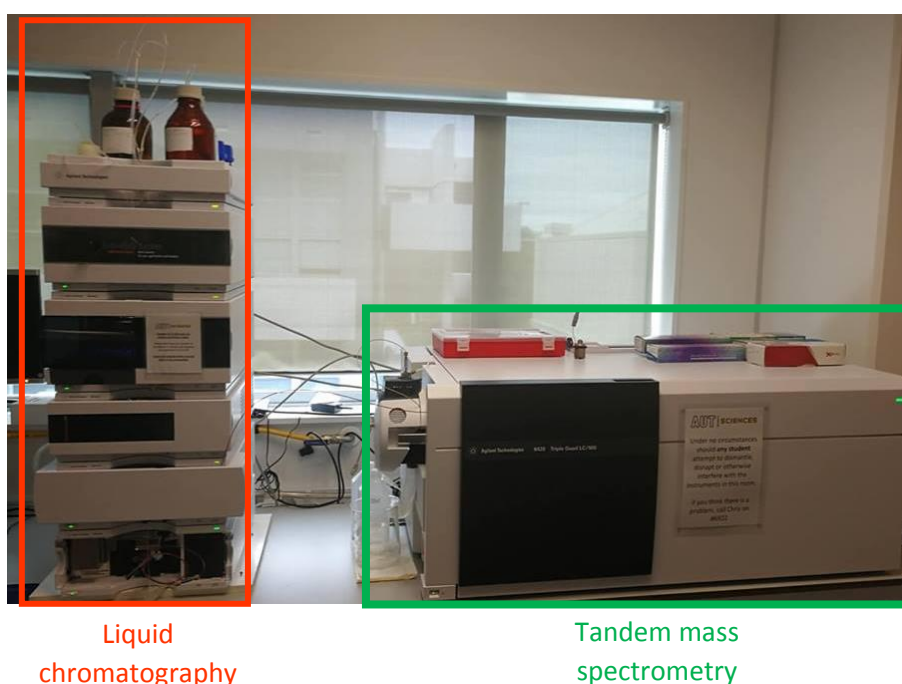


Figure 4. Liquid chromatography combined with tandem mass spectrometer

1.6 Brief Introduction to Mass Spectrometry

Mass spectrometry is a powerful analytical technique used for the identification and quantification of known or unknown compounds and molecules. Basically, this technique utilises electromagnetism to manipulate the movement of ions, separating them according to their mass-to-charge ratio $[m/z]$ (El-Aneed, et al., 2009). Three fundamental components are required to form a mass spectrometer, an ionisation source, mass analyser, and a detector. Each is physically separate and kept in a controlled vacuum environment, as illustrated in Figure 5. Some ion source's are not required to be kept in a vacuum, for example Electrospray Ionisation [ESI] operate at atmospheric pressure (Siuzdak, 2004). In the most basic form of a mass spectrometer, target compounds are introduced to the ionisation source in a flow of gas or liquid, where they are ionised by a variety of physical or chemical processes. These ions can then be manipulated by electromagnetic fields which accelerate them towards a mass analyser, where they are separated based on their m/z . Finally, these ions are converted by the detector to an electrical signal so the data can be analysed by a computer using a suitable software. This is displayed in a form of a mass spectrum which illustrates the relative abundance of the ions and their m/z .

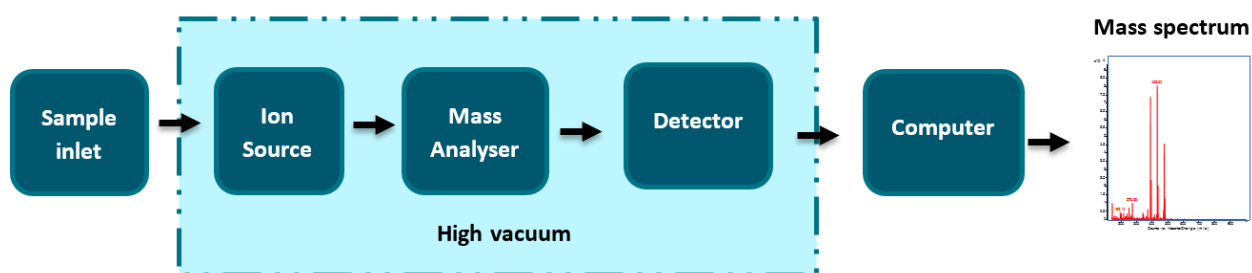


Figure 5. Illustration of a typical mass spectrometer outlining the three main components.

1.6.2 Ionisation Techniques

In mass spectrometry the ions must be in a gas phase, often the conversion is one of the most important steps. Several ionisation techniques have been developed. For simplicity, these techniques can be classed as soft or hard ionisation techniques, where soft ionisation produce little to no fragmentation of the target compound during ionisations and hard methods that produce significant fragmentation (El-Aneed, et al., 2009). For example, Electron Impact Ionisation [EI] is a hard ionisation technique. Electron impact involves the interaction of a beam of electrons produced from a tungsten filament and a flow of gaseous target compounds. This technique is widely used in mass spectrometry, particularly for volatile, thermally stable molecules. Other ionisation techniques have also been developed such as Chemical Ionisation [CI], Matrix-assisted Laser Desorption/Ionization [MALDI], Atmospheric Pressure Photoionization [APPI],

Atmospheric Pressure Chemical Ionization [APCI], and Electrospray Ionisation [ESI]. The latter two techniques are commonly used for analysis of biological compounds such as proteins, DNA, and lipids (El-Aneed, et al., 2009). ESI and APCI are ionisation techniques that will be highlighted since they were used in this research.

Electrospray Ionisation [ESI] is a technique that uses electrical current to convert an aqueous sample into electrically charged droplets at atmospheric pressure (Breitbach, et al., 2015; Ho, et al., 2003). As seen in Figure 6, liquid flows through a thin needle, here droplets are formed, and simultaneously charged due to the electrical current that flows through the needle. The charged droplets are then pulled through a heated capillary, where the solvents are evaporated and concentrated. This leads to unstable droplets which then disperse to form gas phase ions. The ions are then accelerated towards the mass analyser. An advantage of ESI is that ions with multiple charges can be produced. This means instruments with relatively low mass range can be used with ESI to analyse large molecules (El-Aneed, et al., 2009; Siuzdak, 2004). With ESI a wide range of masses can be analysed from very low to millions of Da (Siuzdak, 2004). The ability for ESI to ionise target compounds in solution, allows it to be easily coupled with separation techniques, such as High-Pressure Liquid Chromatography [HPLC] or capillary electrophoresis (Siuzdak, 2004). However, ESI has a low tolerance for impurity. This means the sensitivity can be easily affected by the presence of contaminants, salts, and even complex biological mixtures (Siuzdak, 2004)

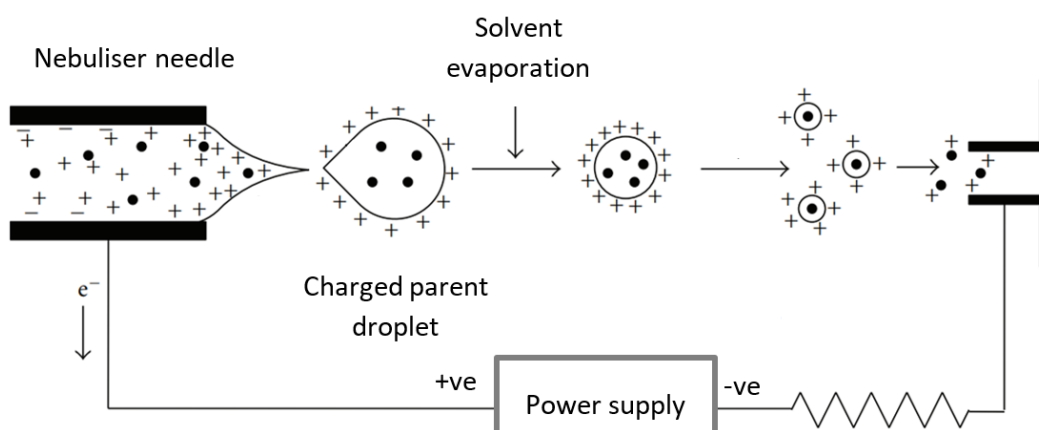


Figure 6. Illustration of ESI producing protonated ions (Banerjee & Mazumdar, 2012)

Atmospheric pressure chemical ionisation [APCI] is another technique that can be used to produce ions at atmospheric pressure. Like ESI, APCI can generate ions directly from the aqueous sample, but they have a different ionisation mechanism (Siuzdak, 2004). In APCI, the formation of droplets and evaporation of the solvent all occur at the nebulizer needle which is between two heating elements, from here the droplets are released in their natural form. The ionisation of the droplets occurs at the region of the corona needle,

as seen in Figure 7. Electrons from the corona needle are ejected into the aerosol, here the molecules are ionized by charge exchange or proton transfer. Unlike ESI, APCI has a relatively high tolerance to the presence of impurities, salts, and also a complex sample matrix (Awad, et al., 2015). However, in APCI there are limited fragments produced during ionisation, and often difficult to detect multiply charged ions (Siuzdak, 2004). APCI is a technique suitable for molecules which have relatively low polarity (Awad, et al., 2015; Siuzdak, 2004).

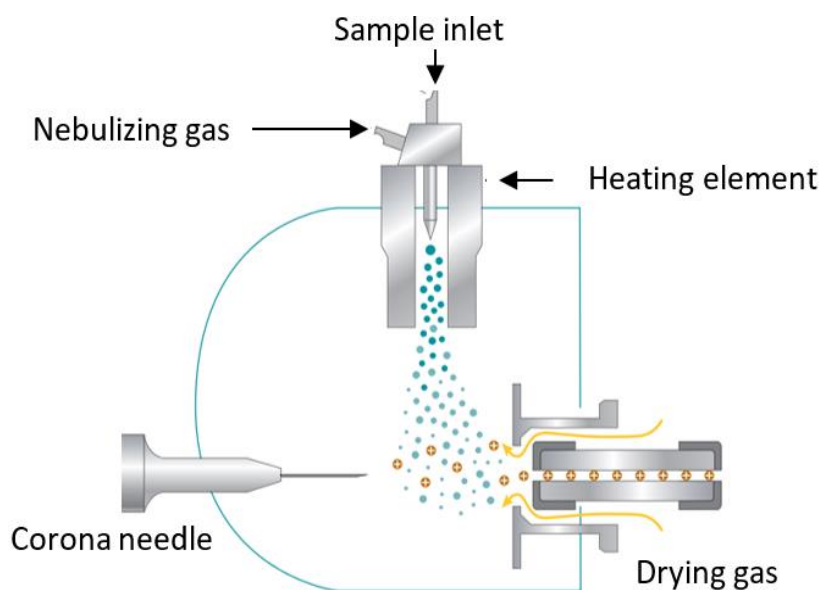


Figure 7 . A schematic diagram of an APCI ionisation source

Early mass spectrometry proved to be a useful tool in the identification and characterization of known or unknown compounds and molecules. However, the instrument was only capable of one stage mass analysis. This meant that structural information of a target analyte relied heavily on the dissociation of molecular ions, which was further limited to the ability ion source. The development of several different ionisation techniques extended the application of the instrument to larger and more complex analytes. However, these ionisation techniques mainly produce protonated or deprotonated species with little or no fragmentation. Consequently, tandem mass spectrometry has emerged as a vital technique in structural analysis used in a wide range of disciplines such as pharmaceutical, environmental, analytical chemistry etc.

1.7 Tandem Mass Spectrometry

Tandem mass spectrometry [MS/MS] was first discovered in the early 1950s (Fenselau, 1992). MS/MS involves the connection of two or more mass spectrometers to obtain a more detailed profile on the structure of target analytes. There are several configurations of MS/MS including time-of-flight-time-of-flight [TOF-TOF], quadrupole-TOF, and triple quadrupole [QQQ]. The advantage of MS/MS is the variety of scan techniques that can be used for different tasks. These include, Product Ion scan [PIS], Precursor Ion, Neutral Loss [NL], Selective Ion Monitoring [SIM], and Multiple Reaction Monitoring [MRM]. The most common scan is the PIS, this involves the selection of a specific ion using the first quadrupole [MS^1], the ion is accelerated to the second quadrupole to be fragmented. The fragments produced are then analysed in the final quadrupole [MS^2]. Precursor ion scan is essentially the reverse scan mode of the product ion scan. Here the third quadrupole scans for a preselected product ion mass that is produced from the collision cell inside the second quadrupole, and the first quadrupole scans and records all precursor ions that generate that specific product ion. Precursor ion scan is a useful technique for identifying compounds that produce similar fragments in a complex mixture. The NL scan, employs both MS^1 and MS^2 to simultaneously scan for the PIS and precursor ion that have lost a neutral fragment. Like natural loss scan, SIM and MRM utilise MS^1 and MS^2 to monitor both the PIS and precursor ion that fragments a preselected ion. Figure 8 provides a visual summary of the different scan modes.

Generally, the quantification of low level SGs in a biodiesel is a challenge when using a single MS with GC or HPLC, as often the target ions are present at or below the chemical noise of the spectra. Tandem mass spectrometry has proven to be effective at characterising SGs and ASGs, as the ions can be further fragmented which aids in distinguishing the target ions from the background noise of the spectra (Schrick, et al., 2011). Also, with the added simplicity of the analysis, where no pre-sample treatments are used like derivatisation, makes MS/MS analysis of SGs superior to chromatography techniques (Schrick, et al., 2011; Wewer, et al., 2011). In this study the QQQ was used to analyse the SGs.

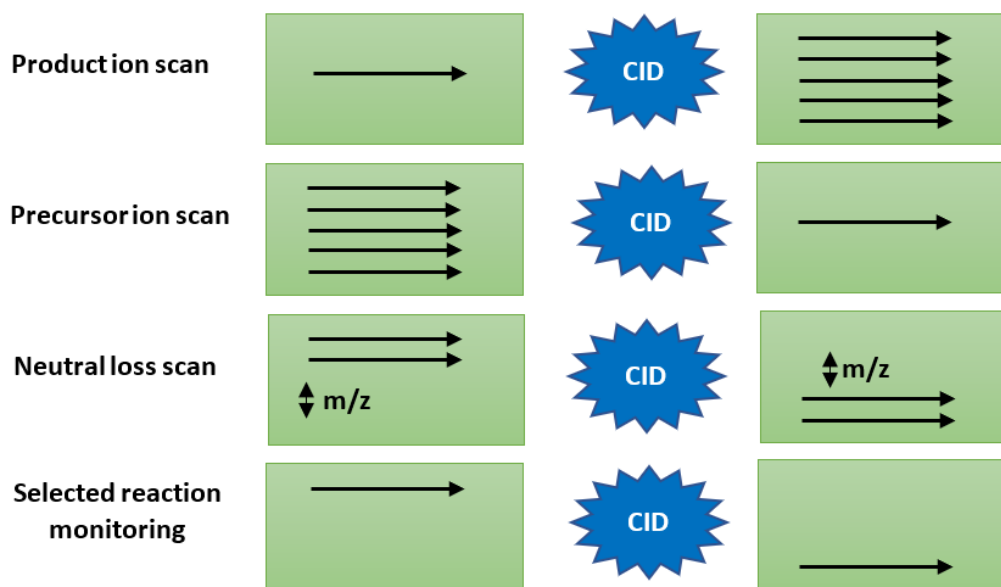


Figure 8. A simple illustration of the different scan modes used in tandem quadrupole. For this study, Collision-Induced Dissociation [CID] was used to fragment the ions in the second quadrupole.

1.8 Sterol Glucoside

Sterol glucosides [SGs] have gained a reputation for their destructive nature in diesel engines. As mentioned previously, SGs and acyl sterol glucoside [ASGs] are naturally present in plants (Schrick, et al., 2011). After transesterification, ASGs are converted to SGs by replacing the hydrocarbon chain with a hydroxyl group. As a result, the concentrations of SGs in biodiesel are generally higher than that found in the feedstock (Wang, et al., 2009). At low temperatures, SGs precipitate to form a suspension of particles which clog the pores of filters and forms deposits at the bottom of fuel tanks and lines, thus preventing the flow of fuel (Songtawee, et al., 2014). The removal of these waxy crystals is almost impossible due to their high melting point of 240 °C and poor solubility in fuel (Lee, et al., 2007). Sitosterol glucoside [SiGluc], campesterol glucoside [CaGluc], and stigmasterol glucoside [StGluc] are the three SGs identified in plant-biodiesel (Monirul, et al., 2015; Peiru, et al., 2015; Hoed, et al., 2008). Structurally, the SGs vary slightly with an extra methyl group or an added double bond, as seen in Figure 9. Therefore, characterising and quantifying the SGs by column chromatography can prove challenging and may require the assistance of advanced analytical instrument. For example, a Nuclear Magnetic Resonance [NMR], High-Resolution Mass Spectrometer [HMS] like Time-of-Flight [TOF], Quadropole-Time-of-Flight [QTOF], and Orbitrap. Or a low-resolution analyser such as a Tandem-Mass Spectrometer [QQQ].

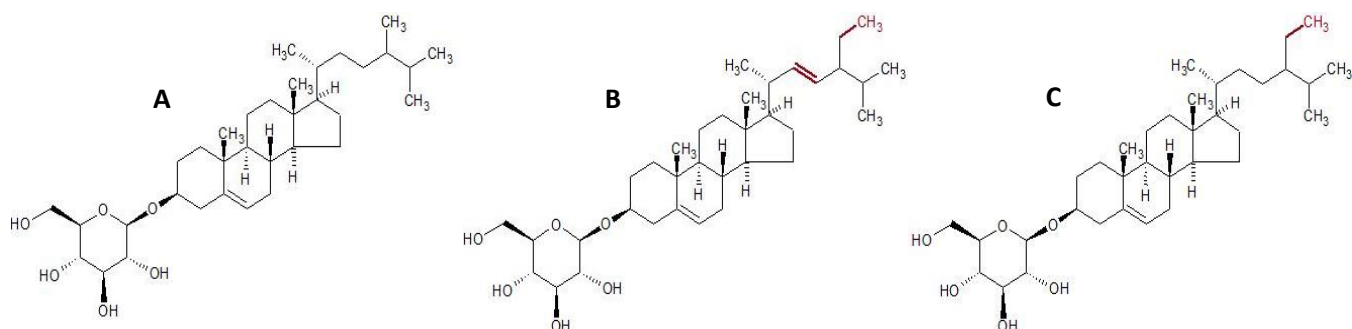


Figure 9. Chemical structure of campesterol glucoside (A), stigmasterol glucoside (B), and sitosterol glucoside (C).

1.8.2 Techniques for sterol Glucoside Analysis

The presence of SGs in vegetable oils is well-known with reports dating back to the mid-20th century. Early works on method development in identifying the SGs included that of Harry Braus and colleagues, who developed a novel method to determine the identity of the white precipitate that formed during the storage of whiskey, which was confirmed to be sitosterol glucoside. This was achieved by thin layer chromatography followed by infrared spectrometry (Braus, et al., 1957). A more detailed report was released in 1973 by Knights, who discussed the derivatisation of SGs by gas chromatography with a mass spectrum [GC-MS] (Knights, 1973). The mass spectrum was presented for the different SGs derivatives, including that of trifluoroacetate [TFA], heptafluorobutyrate [HFBu], and trimethylsilyl [TMS]. In 2004, trace analysis of SGs in dietary food was determined by solid phase extraction [SPE], and GC-MS by silylation (Phillips, et al., 2005).

GC-MS by silylation was modified to confirm the presences of SGs in biodiesel. Van Hoed, et al., 2008, discussed in detail the structural composition of both derivatised and un-derivatised SG by NMR and GC-MS. They reported the concentration of SGs in palm-biodiesel, which ranged from 55 to 275 ppm, and around 158 ppm for soy biodiesel (Hoed, et al., 2008). Paolo Bondioli and colleagues reported SGs concentration in palm-biodiesel to be 160 ppm and 38 ppm for soy-biodiesel. This was achieved by SPE, TMS-silylation by GC-MS. A multistep temperature program was used with initial temperatures of 80 °C to final temperatures of 370 °C (Bondioli, et al., 2008).

Moreau, Scott, and Haas developed a method to determine SGs levels at different stages of biodiesel production. Both normal and reverse phase methods for high-pressure liquid chromatography [HPLC] with an ultra violet [UV] detector, and MS with an evaporative light-scattering detector [ELSD] were reported (Moreau, et al., 2008). Wang and colleagues describe the analyses of SGs in soy-based biodiesel by HPLC-ELSD after centrifugation rather than the use of SPE (Wang, et al., 2009). Figure 10 contains a HPLC chromatogram of a biodiesel sample with emphasis on the sterol glucoside peak. The added advantage of

this method, is the use of a high loaded C18 column which has a higher sample load capacity. This means biodiesel with low concentrations of SGs can be injected at a greater volume. However, this method is only applicable to samples with SGs concentration of 30 ppm or greater. More recently, Songtawee et al (2014), confirmed the presence of ASG and SG in biodiesel by HPLC and fourier transform infrared spectrometer [FTIR]. Surprisingly, they reported levels of ASGs greater than SGs, 202 ppm to 33ppm, respectively in biodiesel. One would expect after the transesterification reaction that ASGs would have been converted to SGs and that ASGs would have been detected at trace concentrations, if at all.

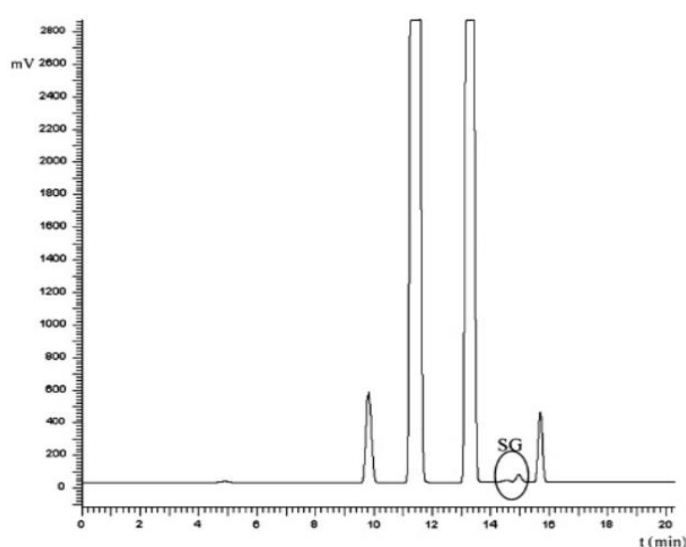


Figure 10. HPLC chromatogram of biodiesel, highlighting the peak for sterol glucoside (Wang, et al., 2009)

An alternative strategy was proposed by Wewer et al, who studied the mass spectrum of ASGs and SGs in plant tissues by nanospray ionization quadrupole-time-of-flight mass spectrometry [Q-TOF MS] (Wewer, et al., 2011). The primary fragments for SGs are observed at mass 383 for campesterol glucoside [camp-Gluc], 395 & 399 for stigmasterol glucoside [stig-Gluc], and 397 for SiGluc. This is due to in-source fragmentation at the ether bond between glucose and sterol, yielding a sterol ion. However, differentiation between isomers was not possible as no chromatographic separation was used (Wewer, et al., 2011). Rico Cha´vez-Santoscoy and co-workers used HPLC-TOF-MS to determine the effects of SG on lipid metabolism (Cha´vez-Santoscoy, et al., 2014). Van Gerpen et al, 2001, employed a matrix assisted laser desorption ionisation time of flight mass spectrometer [MALDI-TOF-MS] to confirm the presence of SG in biodiesel (Gerpen, et al., 2011). The mass spectrum for the different isotropic pattern was presented. Nowadays, the combination of liquid chromatography [LC] and MS has revolutionised the approach for trace analyses of organic compounds. With modern MS offering high selectivity and sensitivity combined with LC equipped

with robust and high efficient ionisation source of APCI and ESI (Cappiello, et al., 2008). This has led to LC-MS becoming a well-established analytical technique in several sectors, to list a few including, environmental science, pharmaceutical, forensic science, and clinical research. As previously mentioned, Moreau et al (2008), identified SGs in biodiesel using reverse phase LC-MS. From the mass spectrum they observed three distinctive ions m/z 383, 395, and 397 which corresponds to CaGluc, StGluc, and SiGluc, respectively. Unfortunately, the detection limit for SG was around 100 ppm, while others have found 60 to 20 ppm of SGs in biodiesel (Pfalzgraf, et al., 2007; Songtawee, et al., 2014). Kathrin Schrick et al (2012), characterised SGs and ASGs in Arabidopsis seeds by direct infusion onto an Electrospray Ionization Tandem Mass Spectrometer equipped with a triple quadrupole. From mass spectrum, they were able to analyse the structure of intact-SGs and ASGs by the neutral loss of hexose moiety in positive mode. However, just like Wever et al, (2011), no chromatographic technique was used which makes identifying the isomers a challenge. In this study we aspire to develop a method for analysing low levels SGs in biodiesel by combining LC with a Tandem Mass Spectrometer [MS/MS] that has a triple quadrupole.

Thesis Objectives

The aim of this research was to develop and validate a simple, specific and sensitive method for the identification and quantification of intact sterol glucoside in biodiesel derived from tallow using LC-MS/MS. The LC-MS/MS method was developed, optimized, and validated for a rapid and accurate analysis of the SGs. In this thesis, chapters 2 to 5 describe how the methodology evolved.

Chapter 2 Analysis of native sterol glucoside by LC-MS

2.1 Introduction

To quantify the SGs in biodiesel fuel is a daunting task, due to their problematic concentration and their compatibility with the fuel. Sterol glucoside have a low volatility and poor ionisation properties, which often requires derivatisation by silylation prior to analysis (Bondioli, et al., 2008; Hoed, et al., 2008). In addition, SGs are relatively non-polar except for the hydroxyl groups on the sugar moiety, so SGs are often encountered in a complex matrix with interfering compounds like FAMES in biodiesel or phospholipids in lecithin (Gerpen, et al., 2011; Montpetit & Tremblay, 2016). Therefore, the SGs are often challenging to separate from their matrix chromatographically. Currently, the two most common techniques used to identify and quantify SGs are gas chromatography [GC] and high-pressure liquid chromatography [HPLC]. Analysis through GC requires SGs to be chemically modified to increase their volatility. This can involve, derivatisation or acid hydrolysis to liberate the sterol moiety, which can then be independently quantified by GC. The drawbacks of derivatisation are that, it often requires considerable time and effort. Acid hydrolysis to separate the sugar or sterol moiety is also protracted and, could make the precise identity of the SGs impossible to determine (Schrack, et al., 2011). As an alternative, intact SGs and ASG have been detected by both normal and reverse-phase HPLC (Moreau, et al., 2008). Both techniques can distinguish SGs species. However, UV absorbance and Evaporative Light Scattering detector [ELSD] are limited in sensitivity. In this chapter, we describe a method for SG analysis using reverse phase liquid chromatography with tandem mass spectrometry [LC-MS/MS] with the aim of identifying and quantifying low levels of both SGs and ASGs. Due to the low concentration of SGs in biodiesel and the challenging nature of the matrix we initially developed our analytical methods for SGs and ASGs in lecithin. Lecithin is a crude biological extract comprised mostly of a complex mixture of phospholipids but also significant quantities of SGs and AGS (Moreau, et al., 2008).

2.2 Experimental

2.2.1 Materials

Samples of tallow-derived-biodiesel and tallow, were obtained from Independent Petroleum Laboratory [IPL], located at Marsden Point, NZ. In this chapter, two biodiesel samples were analysed; 493623 [A] a colourless liquid; 4170117 [B], a pale-yellow liquid, as seen in Figure 11. Soy based lecithin was bought from Countdown supermarket, located at Queen Street, AKL, NZ. Sterol glucoside [mix SGs] with a purity of >98% was obtained from Matreya, reported to contain 55% of sitosterol glucoside, 24.6% campesterol glucoside, 18% stigmasterol glucoside, and 1.4% avenasterol (Matreya LLC, 2018). Unfortunately, due to cost restriction no ASG standard was used in this research. Cholesterol β -D-glucoside standard (>97%), and all solvents used were obtained from Sigma Aldrich (Sigma-Aldrich, 2018). Due to the expense of authentic analytical standards for the compounds targeted in this analysis it is intended to use cholesterol glucoside as a surrogate quantitative standard for the other sterol glucosides.



Figure 11. Tallow based biodiesel, obtained from Independent Petroleum Laboratory [IPL].

2.2.2 Instrumentation

The LC-MS/MS system was an Agilent 1260 Infinity Quaternary LC System (model number: G1311B), composed of different components. This includes a quaternary pump 1260, diode array detector, 1260 infinity ALS sampler (model number: G1329B), 1200 series auto sampler thermostat FC/ALS/Therm (model number: G1330B), and 1260 infinity TCC column component (model number: G1316A). Mass spectrometry was carried out using a 6420 Triple Quadrupole LC/MS System with multimode ionization (MMI) interface source (model number: G1978B). For the column, a high carbon load reversed phase Agilent Poroshell 120 EC-C18 (2.1 x 150 mm, 2.7 μm) was used with an Agilent Poroshell guard column 120 EC-C8 (2.1x5mm, 2.4 μm). Data were collected and analysed on a PC with a MassHunter Acquisition Software. Method development in this study is result driven, as such two methods with different instrument parameters and mobile composition are presented in this chapter.

2.2.3 Mobile Phase

The mobile phase used in this chapter were three different solvent mixtures, labelled as A, B, and C. Solvent A consisted of LCMS grade acetonitrile [MeCN] with an added 0.1% of acetic acid. Solvent B was a mixture of 80% acetonitrile with water, 10mM of concentrated ammonia solution [NH₃] and 0.1% acetic acid. Solvent C was composed of 80% isopropanol [IPA], 20% MeCN, 10mM of ammonia [NH₃] and 0.1% acetic acid. Besides buffering the pH of the mobile phase these additives increased sensitivity in the mass spectrometer by facilitating ionisation and promoting the formation of acetic adducts (Kamel, et al., 1999; Leitner, et al., 2007). Two gradient system were investigated in this chapter to optimize separation, included a binary and a ternary gradient. The final separation conditions were arrived at by a series of trial-and-error runs of standards and lecithin samples.

2.2.4 Methods

2.2.4.1 Preparation of Samples and Standards

Stock solutions for both sample and standard were prepared as described; 10 g/L of Lecithin was dissolved in Methyl tert-butyl ether [MTBE]; 5 g/L of mixed sterol glucoside and cholesterol glucoside were separately dissolved with methanol and chloroform (2:1, v/v). Working solution for the biodiesel samples were diluted to a concentration of 100 mg/L in 80% isopropanol [IPA] before direct injection in the LC-MS/MS. The standard curve was made as follows; Standard A, composed of equal volumes of cholesterol glucoside standard, and mix SGs standard. Both with a concentration of 5000 mg/L. From this 500 µL was subsampled into a separate vial and made up to 1 mL using 80% IPA. This is standard B with a concentration of 2500 mg/L. This was repeated until a total of 6 standards were obtained, with standard F being the lowest concentration of 156 mg/L. In this chapter, no attempts were made to further purify the SGs in the lecithin, tallow, and biodiesel samples. All samples and standards were stored at -4 °C.

Method A

The mass spectrum parameters are as described. The gas flow was 5 L/min at 325 °C, APCI heater of 200 °C, nebulizer was kept at a pressure of 50 psi, and capillary voltage of 2000 volts. The full scan mass spectra were split into two sectors of scan ranges, with the aim of increasing sensitivity. The first scan was acquired from m/z 590 to 650 for SGs, and m/z 850 to 910 for ASGs. Both had a dwell time of 500 seconds. In this method, the mass spectrometry was carried out in negative mode. Table 3 shows the parameters for the solvent gradient. A 10 µL volume of 100 mg/L lecithin was injected into the LC-MS/MS.

Table 3. Gradient elution used to Separate the ASG by liquid chromatography

Time (min)	Flow rate (mL/min)	% Solvent B (10%MeCN, 10Mm NH3, 0.1% acetic acid)	% Solvent C (80% IPA, 20% MeCN, 10Mm NH3, 0.1% acetic acid)
0.01	0.4	0	0
0.01	0.05	75	25
2.00	0.05	60	40
2.50	0.05	40	60
10.00	0.05	35	65
10.40	0.05	0	100
11.00	0.05	0	100
12.00	0.05	75	25

Method B

The mass spectrum are as follows; full scan range were between m/z 580- to 645 in negative mode with a dwell time of 500 seconds. Source parameters; gas temperature was set at 300 °C; APCI heater 200 °C; gas flow 5 mL/min; nebulizer 50 psi; capillary voltage of 2000 V was used. A 10 µL injection volume was used. Table 4 illustrates the gradient elution for the separation of the SGs. Table 5 lists the conditions for selection ion monitoring [SIM].

Table 4. Elution gradient used for the separation of SGs by LC-MS

Time (minute)	% Solvent A (MeCN, 0.1% acetic acid)	% Solvent B (10%MeCN, 10Mm NH3, 0.1% acetic acid)	% Solvent C (80% IPA, 20% MeCN, 10Mm NH3, 0.1% acetic acid)
0.01	80.00	20.00	0.00
0.40	80.00	20.00	0.00
6.00	30.00	10.00	60.00
6.80	90.00	10.00	0.00
7.50	80.00	20.00	0.00

Table 5: Parameters used for Selective Ion Monitoring of sterol glucosides

Analyte	Precursor Ion	Product Ion	RT	Ion Polarity
Campesterol-glucoside	621.4	621.4	6.849	Negative
cholesterol glucoside	607.4	607.4	6.055	Negative
sitosterol glucoside	635.5	635.5	7.673	Negative
stigmasterol glucoside	633.4	633.4	7.096	Negative

2.2.5 Method validation

As part of method validation, six different concentrations of the standards were analysed. The peak area, also referred to as response, of the six standards were plotted against their corresponding concentration (mg/L). The optimized elution gradient used in Method B, seen in Table 4, and mass parameters for SIM analyses in Table 5 were the optimized condition used. In order to determine the sensitivity of the LC-MS/MS the limits of detection and limits of quantification were calculated, this was achieved using the Excel software. For simplicity, signal-to-noise and the concentration of the standards were used to estimate the LOD and LOQ by multiplying it by a factor of 3 and 10, respectively. The methods detection limits [MDL] were determined by multiplying the LOQ with the dilution factor.

A calibration of cholesterol glucoside was used measure the concentration of SGs in the samples. The concentration of the SGs in the samples were measured according to the calibration curve of cholesterol glucoside, this ranged from 500 mg/L to 15.62mg/L. The slope obtained from the concentration and signal-to-noise ratio of the standard were used to measure the detection limits [LOD] and quantification limits [LOQ], by the multiplying the slope by a factor of 3 and 10, respectively. To measure the sensitivity of the method, we estimated the detection limit of the method [MDL] by multiplying the LOQ by the dilution factor.

2.3 Results

To optimize the methodology for the analysis of the SGs by LC-MS/MS, we evaluated several different conditions and their effects on the separation and ionization efficiency of the SGs and ASG species. Firstly, the parameters for the mass spectrum were modified to obtain the highest intensity of underivatized ASGs and SGs, with campesterol glucoside [CaGluc], stigmasterol glucoside [StGluc], and sitosterol glucoside [SiGluc] being the target analytes. Secondly, the mobile gradient was modified to gain the greatest separation between the SGs species and the ASGs species.

The optimal conditions used to detect the underivatized SGs and ASGs in the mass spectrum were assessed by injecting the lecithin solution with a concentration of 100 mg/L to the LC-MS/MS. Originally, the full scan [LC-MS] or total ion count [TIC] was set to scan between the ranges of m/z 540 to 910 in both positive and negative mode. We observed no ASGs or SGs in positive mode but were abundant in negative mode in the form of their deprotonated acetic adduct $[M + \text{HAc} - \text{H}]^-$ and the chlorine adduct $[M + \text{Cl}]^-$. To better illustrate the distinctive patterns of the adducts, a heatmap is used. This is generated using Python software, as seen in Figure 12, 13, and 14. Basically, a heatmap is a graphical representation of the numerical value collected from the TIC spectrum. Each m/z value is presented in the form of colours and their relative abundance is shown in the intensity of the colours. For example, the heatmaps presented in this chapter, show the colours of dark brown, red, orange, yellow, and white, respectively in increasing order of intensity. Dark brown being the low intensity and white is for high concentration of that specific ion. To further enhance the sensitivity, the scan range used in Method A was split into two ranges of 590 to 650 m/z for SGs, and 850 to 910 m/z for ASGs.

On closer examination of the heat maps, we observed three distinctive patterns. Firstly, we observe the acetic and chlorine adducts with a difference of 24 m/z at the same retention time, this pattern can be clearly seen in the heat map for the SGs in Figure 12. The ASGs, on the other hand, are much more diverse in structure, as they vary in both the chain length of their acyl moiety and its saturation. Therefore, distinguishing between the acetic and chlorine adducts can be difficult due to their matching m/z values. The heat map of the ASGs was duplicated to differentiate between acetic adducts (Figure 13) and chlorine adducts (Figure 14). The observed m/z from the TIC correlates with calculated m/z in Table 9. The molecular mass of the ASGs have been reported which included the m/z of their ammonium adduct (Schrick, et al., 2011; Wewer, et al., 2011). Although, we were not able to reproduce this method for analyzing intact SGs and ASGs using positive mode ionisation. The second pattern can be seen in the heat map of the ASGs. Here we observed a linear pattern for each of the ASG species. For example, the acetic adduct of the acylated campesterol glucoside labelled as 9 to 12, seen in Figure 12, is separated by m/z increments of m/z 2. These ion masses correlate with the C18:0 to C18:3 of acyl CaGluc, refer to Table 9. From this pattern, we observe that ASGs with more double bonds on the alkyl chain, will elute out sooner than ASGs with no double bonds.

From the heat map of the ASGs, we also observe that acetylated StGluc with C18:2 showed an intense signal, this was also mirrored in the chlorine adduct labelled 3c. Two different conditions were used for the LC-MS of SGs and ASGs in Figure 11 and 12/13, due to optimizing the gradient system to improve the separation between the SG species. Method A was used for ASGs and Method B was used for the SGs. Lastly, the isotopic pattern for each SG and AGS species with a 1 m/z difference can be seen in the heat maps, each vary in intensity. Figure 15 shows the mass spectrum for cholesterol glucoside [CholGluc], campesterol glucoside [CaGluc], stigmasterol glucoside [StGluc], and sitosterol glucoside [SiGluc]. The patterns observed in Figure 15, is parallel to that seen in the heatmaps. Here we observe the m/z correlating to acetic and chlorine adducts, with the acetic adduct being more abundant, as well as their isotopic pattern.

The calibration curve presented in Figure 16, demonstrated a linear relationship with $y = 212.2x$, with a correlation coefficient $r^2 > 0.995$. The LOD and LOQ were 7 mg/L and 23 mg/L, respectively. To account for the 10000-fold dilution of the biodiesel sample, MDL was estimated to be 234071 mg/L. When this method was applied to the biodiesel samples and tallow, no peaks for SGs or ASGs were seen. For lecithin we were able to measure the concentration of each SGs. In sample of lecithin we measured 5 ng/ug of CaGluc, 9ng/ug StGluc, and 4 ng/ug of SiGluc.

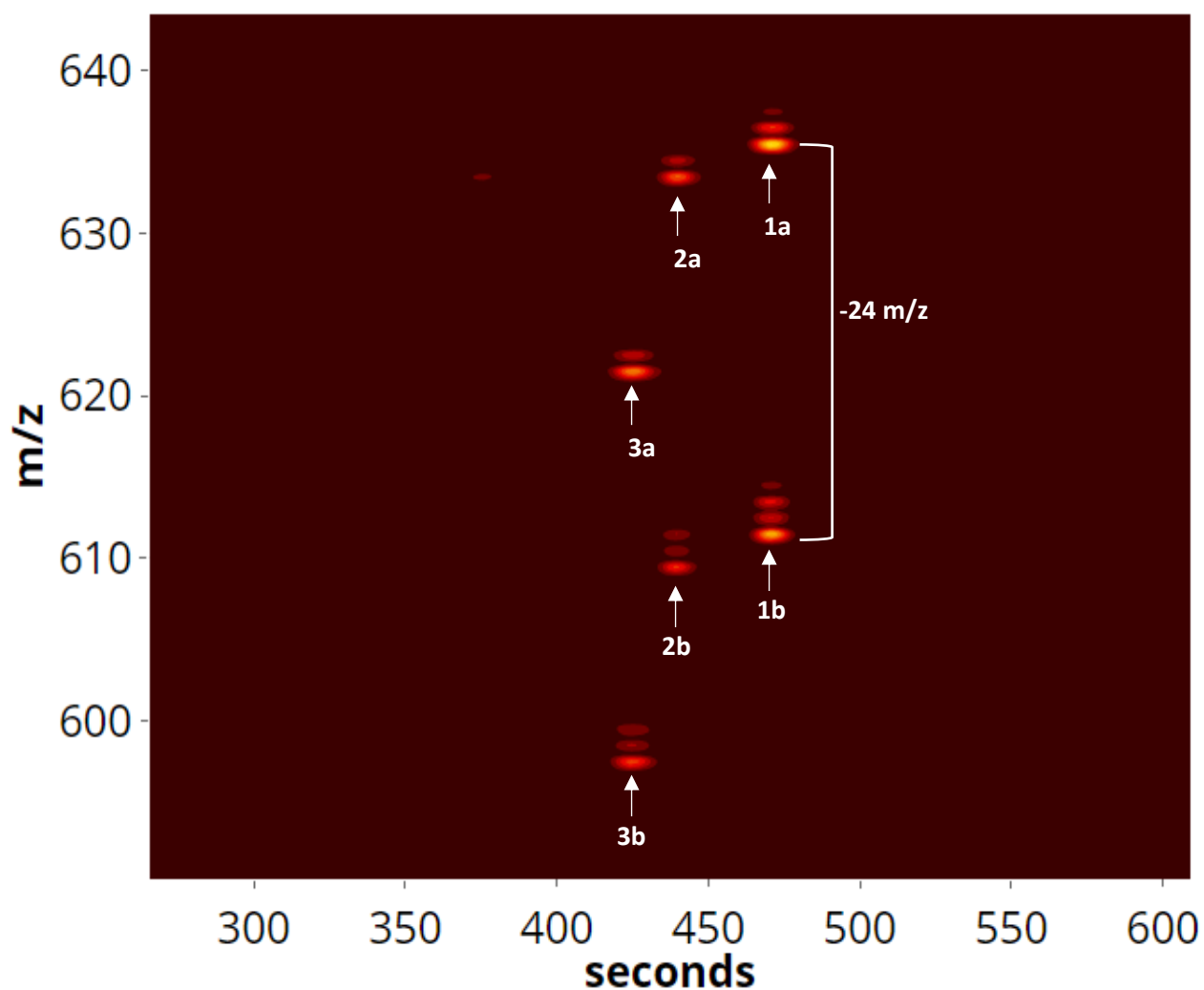


Figure 12. A heat map of the SGs present in Lecithin. This shows the acetic adducts $[M + \text{HAc} - \text{H}^+]^-$, which are labelled with numbers. And the chlorine adducts $[M + \text{Cl}]^-$ are labelled alphabetically, can also be seen to align with the acetic adducts with a difference of m/z 24, as seen in the table below.

Table 6. Identification of the acetic and chlorine adducts for the SGs

	Sitosterol glucoside	Stigmasterol glucoside	Campesterol glucoside
$[M + \text{HAc} - \text{H}^+]^-$	1a	2a	3a
$[M + \text{Cl}]^-$	1b	2b	3b

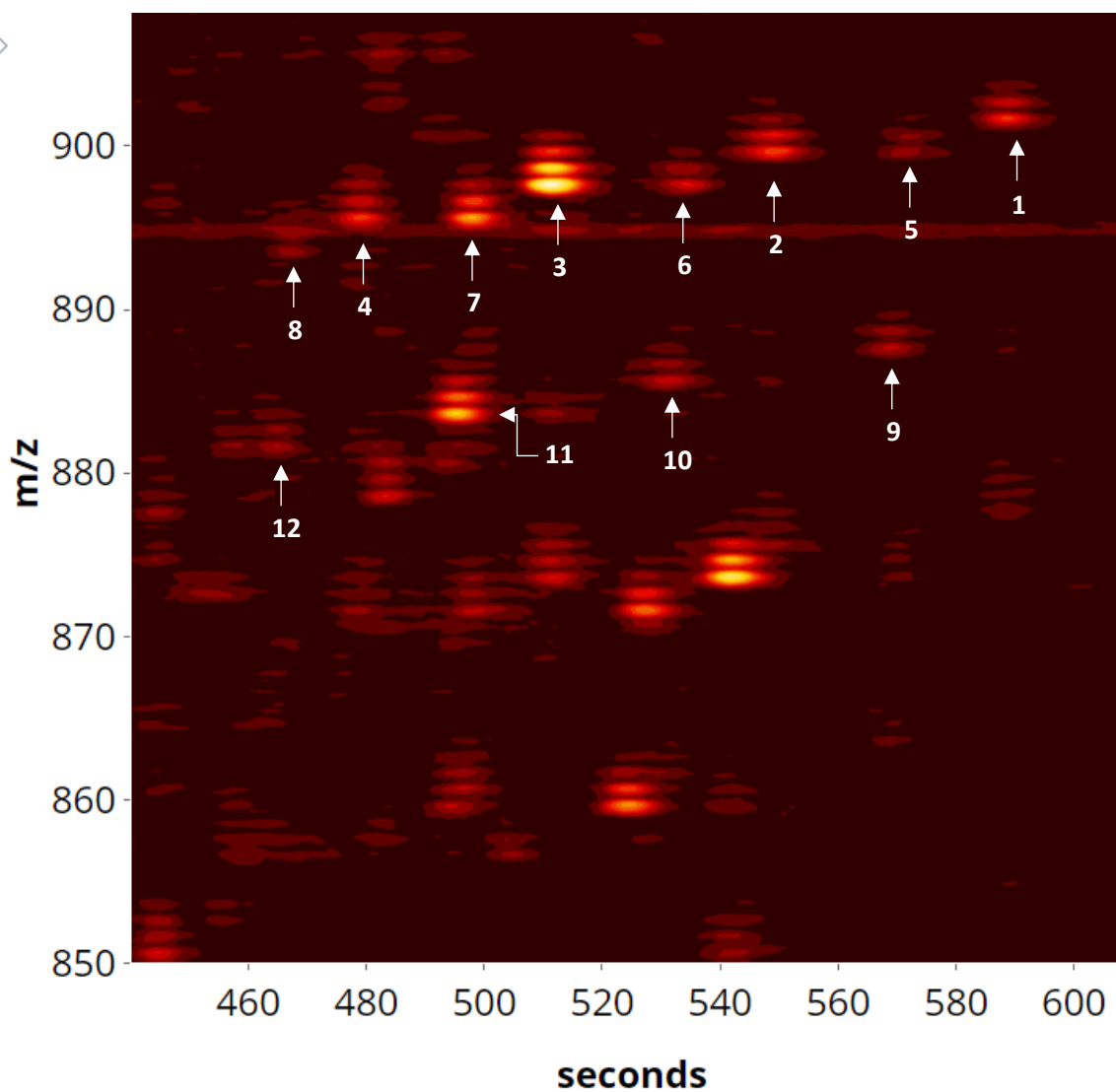


Figure 13. Heatmap of the total ion count for lecithin in negative mode. The scan ranged from 850 to 910 m/z, as described in the experimental section of Method B. The acetic adducts of the ASGs $[M + \text{HAc} - \text{H}]^-$ are highlighted and assigned numbers, as listed in the table below.

Table 7. Characterisation of the acetic adducts of the ASGs

	Sitosterol glucoside	Stigmasterol glucoside	Campesterol glucoside
C18:0	1	5	9
C18:1	2	6	10
C18:2	3	7	11
C18:3	4	8	12

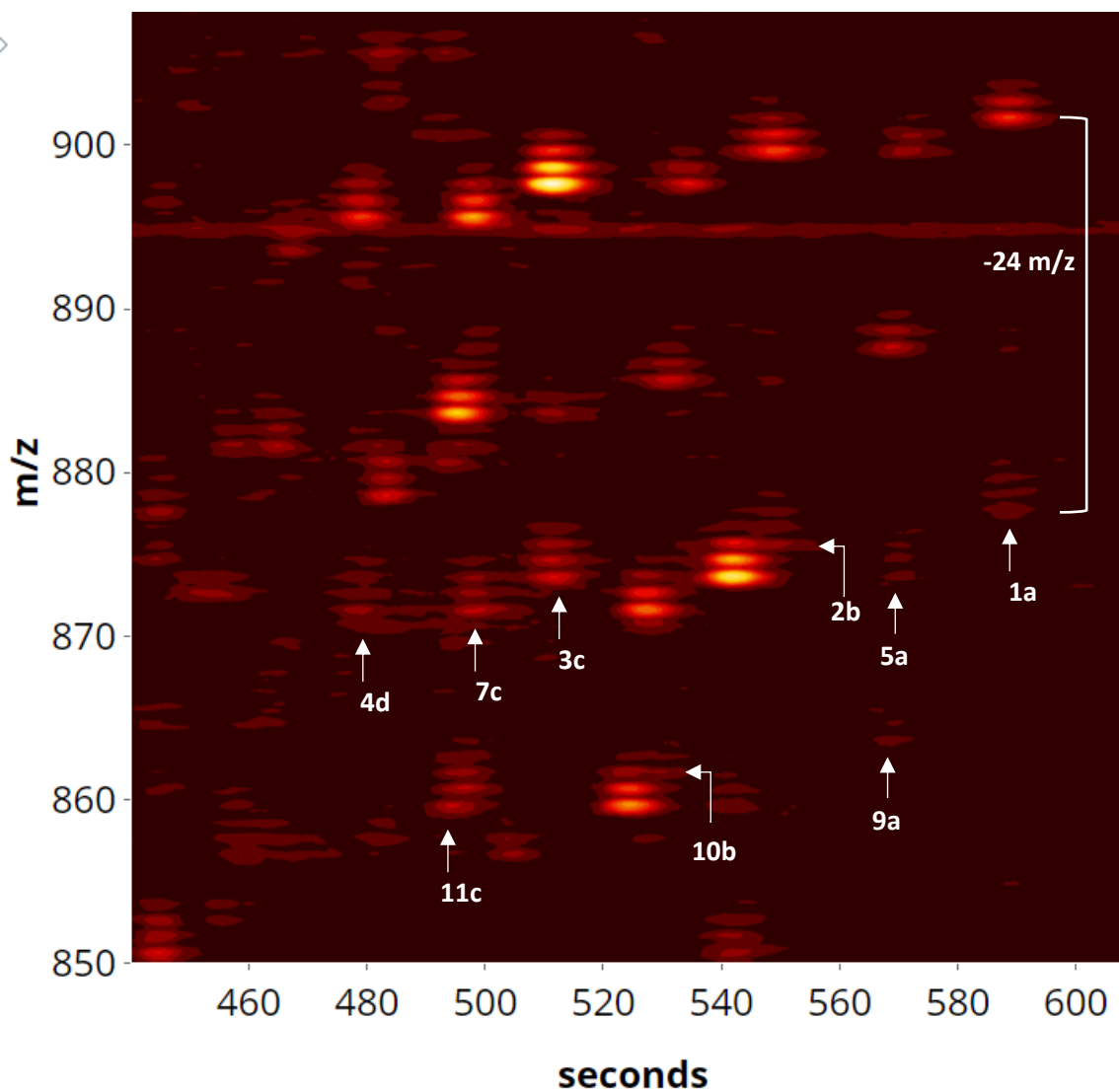


Figure 14. An identical heatmap from Figure 13. This illustrates the chlorine adducts that align with the acetic adduct of the ASGs, with a difference of 24 m/z. From this heat map we can identify the chlorine adduct for the acyl SiGluc.

Table 8. Characterisation of the chlorine adducts of the ASGs

	Sitosterol glucoside	Stigmasterol glucoside	Campesterol glucoside
C18:0	1a	5a	9a
C18:1	2b	-	10b
C18:2	3c	7c	11c
C18:3	4d	-	-

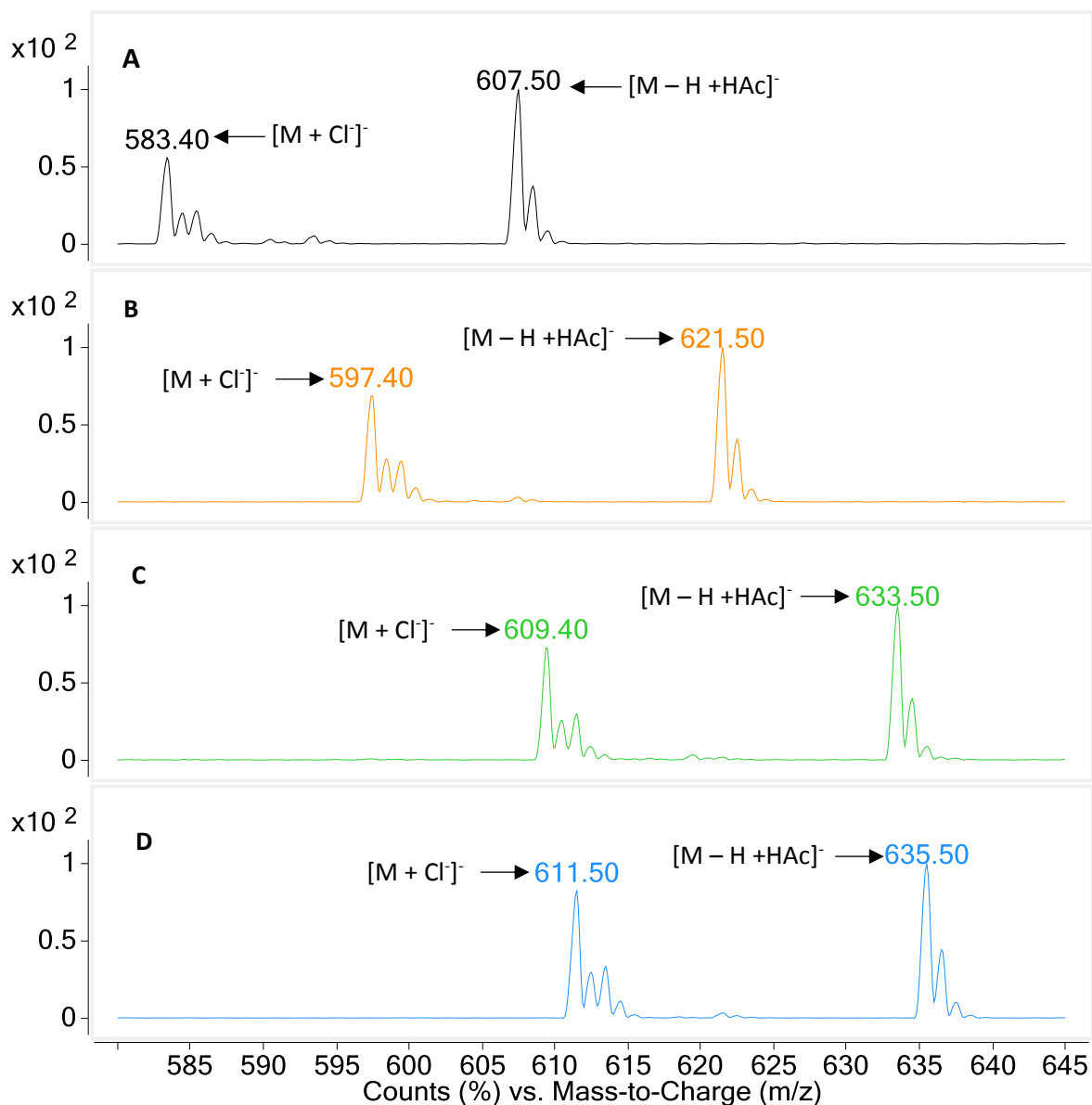


Figure 15. Reconstructed negative ion chromatogram after LC-MS/MS analysis with MS1 set to scanning mode. The mass spectrum for the following SG species are shown with both acetic and chlorine adducts; (A) cholesterol glucoside, (B) campesterol glucoside, (C) stigmasterol glucoside, and (D) sitosterol glucoside.

Table 9. Profile of sterol glucoside and acyl sterol glucoside

	Compound	Formula	MIM	[M + CH₃COOH - H⁺]⁻	[M + Cl]⁻
	Cholesterol glucoside	C33H56O6	548.41	607.42	583.38
	Sitosterol glucoside	C35H60O6	576.44	635.45	611.41
	Stigmasterol glucoside	C35H58O6	574.42	633.44	609.39
	Campesterol glucoside	C34H58O6	562.42	621.44	597.39
ASGs	16:2 Campesterol-Gluc	C50H84O7	796.62	855.64	831.59
	16:1 Campesterol-	C50H86O7	798.64	857.65	833.61
	16:0 Campesterol-	C50H88O7	800.65	859.67	835.62
	18:3 Campesterol-	C52H86O7	822.64	881.65	857.61
	18:2 Campesterol-	C52H88O7	824.65	883.67	859.62
	18:1 Campesterol-	C52H90O7	826.67	885.68	861.64
	18:0 Campesterol-	C52H92O7	828.68	887.70	863.65
	16:2 Sitosterol-	C51H86O7	810.64	869.65	845.61
	16:1 Sitosterol-	C51H88O7	812.65	871.67	847.62
	16:0 Sitosterol-	C51H90O7	814.67	873.68	849.64
	18:3 Sitosterol-	C53H88O7	836.65	895.67	871.62
	18:2 Sitosterol-	C53H90O7	838.67	897.68	873.64
	18:1 Sitosterol-	C53H92O7	840.68	899.70	875.65
	18:0 Sitosterol-	C53H94O7	842.70	901.71	877.67
	16:2 Stigmasterol-	C51H84O7	808.62	867.64	843.59
	16:1 Stigmasterol-	C51H86O7	810.64	869.65	845.61
	16:0 Stigmasterol-	C51H88O7	812.65	871.67	847.62
	18:3 Stigmasterol-	C53H86O7	834.64	893.65	869.61
	18:2 Stigmasterol-	C53H88O7	836.65	895.67	871.62
	18:1 Stigmasterol-	C53H90O7	838.67	897.68	873.64
	18:0 Stigmasterol-	C53H92O7	840.68	899.70	875.65

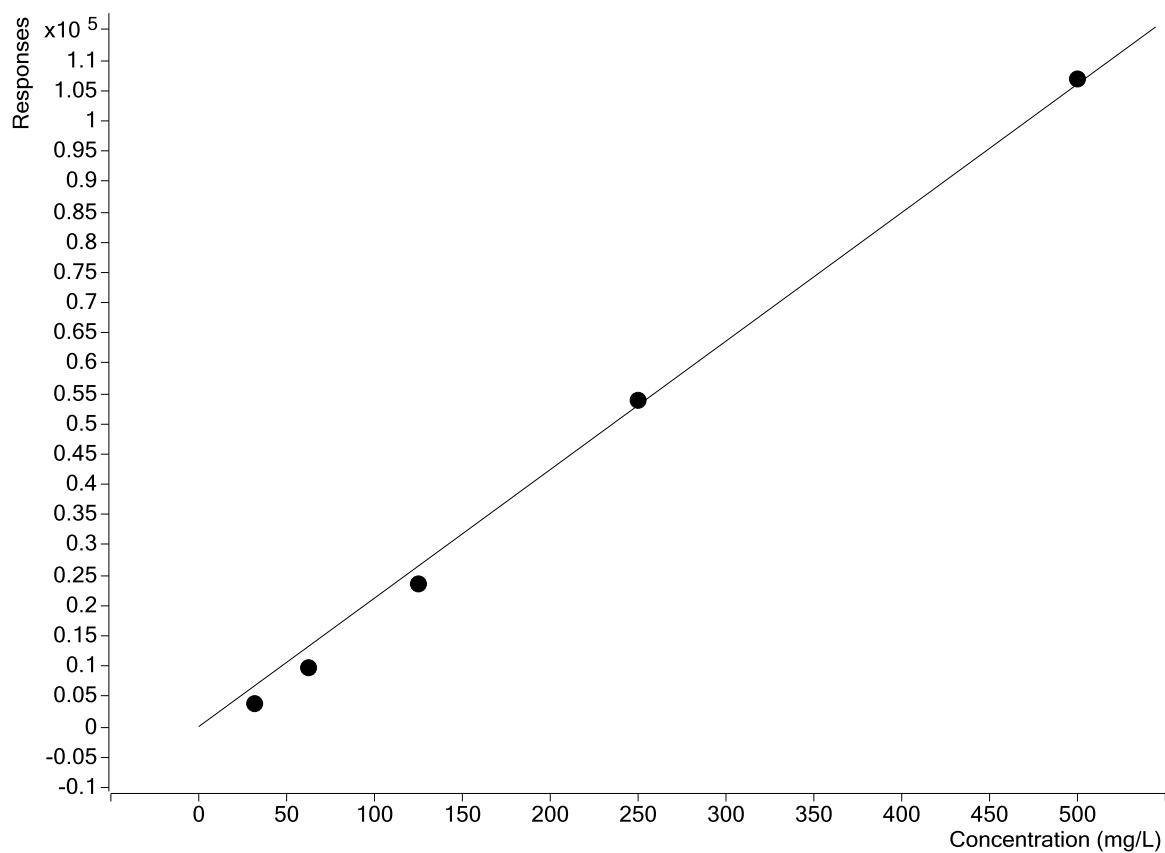


Figure 16. Standard curve of cholesterol glucoside. A linear behaviour can be observed with $y=212.15x$, and a correlation coefficient $r^2= 0.996$

3.4 Discussion

3.4.1 Solvent choice

Biodiesel can contain a wide range of components such as, FAMES, fatty acids, glycerides, SGs, and ASGs. Consequently, the polarity of the compounds varies from polar to non-polar, thus the use of only one solvent is not appropriate to separate the SGs from the biodiesel matrix. Therefore, acetonitrile was selected for compounds that are non-polar, and isopropanol [IPA] was used to dissolve polar compounds. As the Agilent 1260 Infinity Quaternary LC System is equipped with a quaternary pump and a solvent delivery system, this allowed for gradient elution.

3.4.2 Gradient elution

Initially, a binary gradient was used to mirror the conditions required for the analysis of samples by a high-resolution LC-Q-TOF, which only operated with a binary gradient. The goal was to obtain reference data that would allow us to compare our results. Unfortunately, no results were collected due to ion suppression from trifluoroacetic acid, which was used to clean the column in the LC. Nonetheless, the use of internal standard, calibration curve, and mass spectrometry confirmed the identity of SGs and ASGs. The goal was now to find a solvent mixture and separation conditions that produced sufficient resolution while reducing total elution time. The binary gradient was modified to improve the separation of the ASG. However, after several attempts, the separation of the ASGs did not improve and therefore not sufficient enough to allow for Multiple Reaction Monitoring [MRM] or Selective Ion Monitoring [SIM]. These two analyses are highly selective and highly sensitive, which would have replaced the need for pure ASG standard. Ternary gradient system was then used to optimize the separation of the SGs, this allowed for SIM analysis. The optimum condition used to separate the SGs was achieved using the ternary gradient listed in Table 10.

Table 10. Separation condition used in Method B

Solvent B: Acetonitrile with 0.1% Acetic acid			
Solvent C: 10% Acetonitrile, 90% Water, with added 10Mm of concentrated Ammonia and 0.1% Acetic acid			
Solvent D: 80% Isopropanol, 20% Acetonitrile, 10Mm of concentrated Ammonia, and 0.1% Acetic acid			
Flow rate: 0.05 mL/min			
Injection volume: 10 μ L			
Column temperature: 40 °C			
Mobile Phase Gradient			
Time (minute)	% Solvent B	% Solvent C	% Solvent D
0.01	80.00	20.00	0.00
0.40	80.00	20.00	0.00
6.00	30.00	10.00	60.00
6.80	90.00	10.00	0.00
7.50	80.00	20.00	0.00

3.4.3 LC-MS analysis

From the LC-MS, the acetic and chlorine adducts for the SGs and ASGs were more prevalent than the deprotonated ions $[M - H]^-$. Initially, a wide scan range was used to determine the presence of SGs and ASGs in lecithin. After confirming their presence, the scan range was then split into two segments to improve sensitivity of the analysis. For SGs a scan range of 580 to 645 m/z was used, and 850-910 m/z for ASG. Essentially, by reducing the scan ranges we improved the signal-to-noise ratio which in turn increased sensitivity. Full scan of the SGs and ASGs were run in both positive and negative mode. Schrick et al, (2012) had characterised the SGs and ASGs in positive mode. However, in our study we observed no SG in positive mode, only in negative mode for both SGs and ASGs. MassHunter software was used to process the mass spectrum of the sterols. The absorbance of the SGs and ASGs were also evaluated using spectrophotometric detection. According to Moreau et al (2008), SGs can be identified by UV absorbance detection at 205 nm. Unfortunately, no absorbance was detected. Due to the limited scope of the MSc project and our lack of pure ASG standards, method development in this study focused on achieving quantitative and qualitative data for SGs. For a better visualisation of the TIC for both SGs and ASGs, the data collected was configured to produce a heatmap which provided a three-dimensional view of the raw data from full scan. Interestingly, the heatmap showed both the chlorine and acetic adducts that correspond to sterols with the same RT and m/z ratio. The ions' m/z also match the calculated m/z in Table 9. Unfortunately, due to the poor ionisation ability of SGs, no fragmentation was observed during product ion scans. Although, SIM was usefully applied to monitor the acetic adducts of the SGs, thus increasing the sensitivity of the analysis.

Overall, the method developed in this chapter describes how a new LC-MS/MS method can be used for the identification and quantification of sterol glucoside. The LOD and LOQ were estimated to 7 mg/L, and 23 mg/L, respectively. The detection limit of the method was measured to account for the 10000-fold dilution of the biodiesel samples. The high method detection limit [MDL] is a concern and with no traces of SGs in the biodiesel sample, we suspected that diluting the biodiesel sample has significantly reduced the signal sensitivity of analysing the SGs. For this analysis, it was necessary to dilute the sample to make it more suitable for direct injection to the LC-MS/MS. Therefore, we aim to improve this method by increasing the signal of SGs in the biodiesel by derivatising the sugar moiety of the sterol glucoside. This led us to investigate the presences of SGs by the traditional method of analysing with gas chromatography with a mass spectrometer [GC-MS].

Chapter 3 Analysis of sterol glucoside by silylation and GC-MS

3.1 Introduction

As the method proposed in chapter 2 was inadequate for detecting SGs in biodiesel. Therefore, Gas chromatography with mass spectrometry [GCMS] was investigated, as it has been widely used for the analysis of sterol glucoside. Due to their physiochemical properties, derivatisation is often used to make that the SGs volatile for GC analysis. We used the common silylation reagent bis(trimethylsilyl)trifluoroacetamide [BSTFA] to modify the hydroxyl groups of the SGs' sugar moiety with trimethylsilyl groups to achieve this. Silylation has been reported to produce distinctive fragments for SGs (Gutiérrez & del Río, 2001; Knights, 1973; Laine & Elbein, 1971; Phillips , et al., 2005). In this chapter, glucose was used as a positive control to confirm the success of the derivatisation process and to assist in identifying the SG derivatives.

3.2 Experimental

3.2.1 Materials

Samples and solvents used in this chapter were provided from Sigma Aldrich. Stock solution of the samples were prepared as described; 10 g/L of glucose was dissolved in 50% methanol and water, and 5 g/L of cholesterol glucoside was dissolved with chloroform and methanol (1:1 v/v). Working solution were made by diluting the standards to 100 mg/L with 80% isopropanol [IPA].

3.2.2 GC-MS analysis

The analysis was performed using an Agilent 7890B gas chromatography combined with an Agilent 5977B single quadrupole mass spectrometer. The GCMS was equipped with a 30m long fused-silica capillary (DB-5MS; Part No. 122-5532G; 30 m x 0.25 mm, 0.25 μ m film thickness). The oven was heated from 40 °C to 325 °C with no holding time, at a rate of 20 °C/min. The temperature was then held for 40 min at 325 °C. The injector (split-splitless) and the transfer line temperature were maintained at 300 °C. Helium was used as carrier gas, and injection was performed in splitless mode. The split ratio was 5:1 with a flow rate of 5 mL/min. The electron impact [EI] mass spectra was acquired from m/z 48 to 800. The ionisation energy was 70 eV. Both standard compounds were identified by the retention times and interpretation of their mass spectra. Results collected were analysed on a PC with a MassHunter Acquisition Software.

3.2.3 Methods

Prior to GCMS analysis, an aliquot of each sample was evaporated to dryness using a centrifugal concentrator, for a duration of 15 min at 45 °C. The derivatisation agent of bis(trimethylsilyl)trifluoroacetamide [BSTFA] and pyridine was added and left to react at 80 °C for 1hr. Once the solution had cooled, excess BSTFA was removed under a gentle stream of nitrogen gas. The silylated compounds were re-dissolved in 100 μ L methyl tert-butyl ether [MTBE] and transferred into a low-volume insert in an amber, autosampler vial for GC-MS analysis.

3.3 Results

Figure 17 shows a comparison of the total-ion chromatograms for the blank, chol-Gluc and glucose standard, after BSTFA derivatisation. From the graph, we observe a small peak present in the chol-Gluc around 2000 seconds, while glucose has two distinctive peaks around 500 to 600 seconds. The mass spectrum extracted from these peaks showed characteristic fragments for tetra(trimethyl)silyl [TMSi] of glucose and the sugar moiety of a sterol glucoside (Laine & Elbein, 1971; Gutie´rrez & del Ri´o, 2001; Phillips, et al., 2005). However, no molecular ion was observed for both TMSi derivatives. In Figure 18, we observe the TMSi group producing an intense ion signal at m/z 73, 147, 117, 204, 217, and 305. Interpretation of the fragmentation pattern are as follows; m/z 73 and 147 are ions produced from the cleavage of two vicinal TMSi groups; m/z 117 corresponds to the loss of one TMSi and two methylene groups; The loss of three TMSi groups and a methylene correlates with m/z 204; Lastly, m/z 305 is produced from the cleavage of four TMSi groups and a methylene. Furthermore, we observe the relative intensity of m/z 204 compared to m/z 217 which confirms the glucose ring is in the pyranose configuration instead of that of furanose ring, which would have m/z 217 as the prominent than 204 m/z (DeJongh, et al., 1969). Similar fragmentation pattern is reflected in the cholesterol glucoside, seen in Figure 17. However, we were unable to observe the fragmentation for the sterol moiety, possibly due to the relatively high ionisation energy. The base peak of m/z 207 seen in Fig 17, is present in the spectrum of the blank, thus must be classed as a contaminant.

The chromatogram presented in Figure 20 and 21 shows the extracted ion chromatogram [EIC] of the characteristic ions seen in Figure 18 and 19. Interestingly, we observed the EIC peaks have the same pattern seen in TIC and the same retention time window. For example, the EIC of TMSi-glucose all the characteristic ions elute out at the exact same retention time between 500 to 600 seconds. Although, the EIC of cholesterol glucoside only showed two peaks that corresponds with m/z 204 and 217 with the same retention time as the small peak seen in the TIC of cholesterol glucoside. Unfortunately, this means the ions of m/z 73 and 147 were not from the TMSi-cholGluc, thus must be assumed to be an artefact.

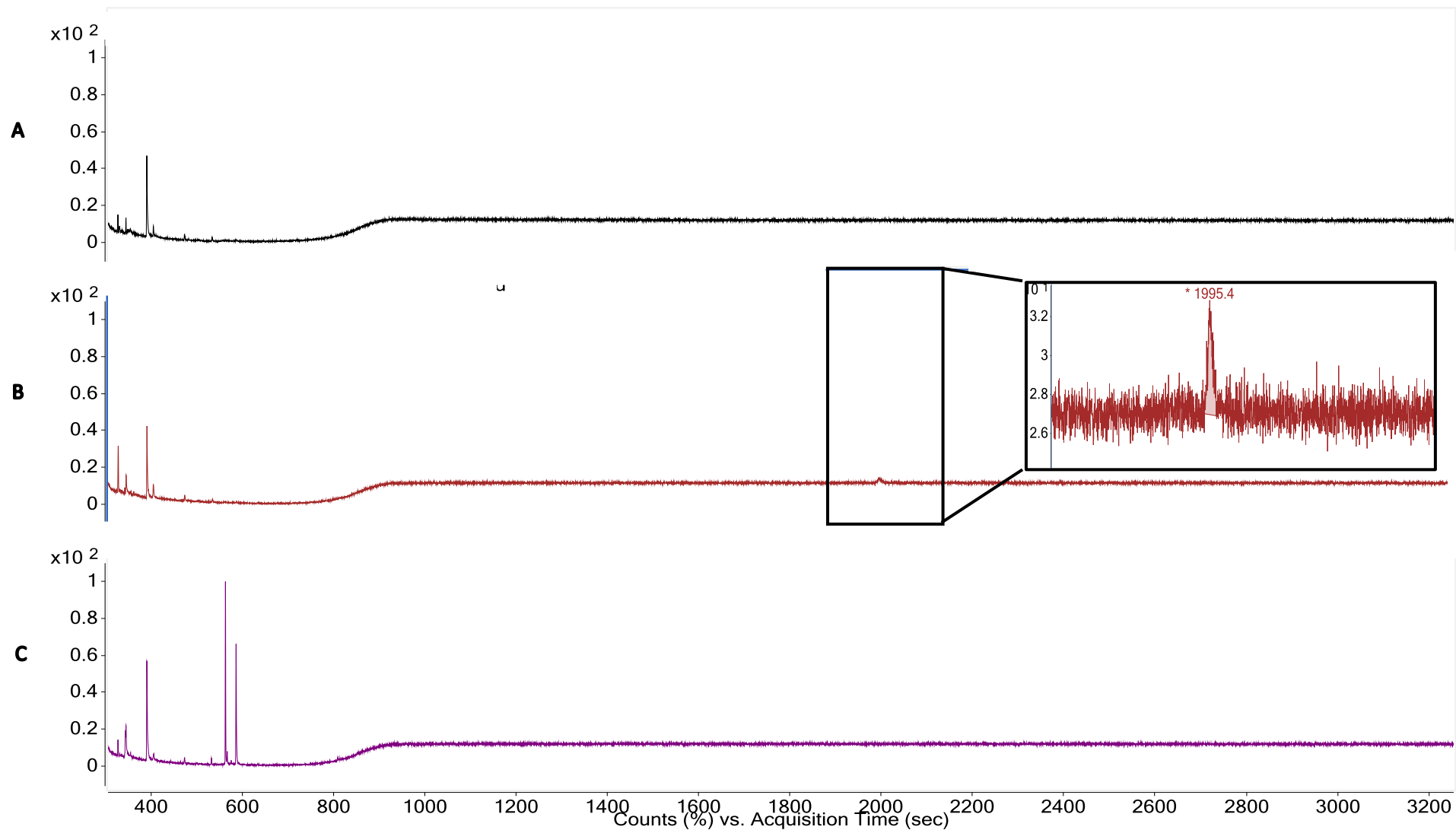


Figure 17. A comparison of the total-ion chromatogram of the blank (A), cholesterol glucoside(B), and glucose (C), after BSTFA derivatization. The inset shows a small peak present in only the cholesterol glucoside scan at 1995 seconds.

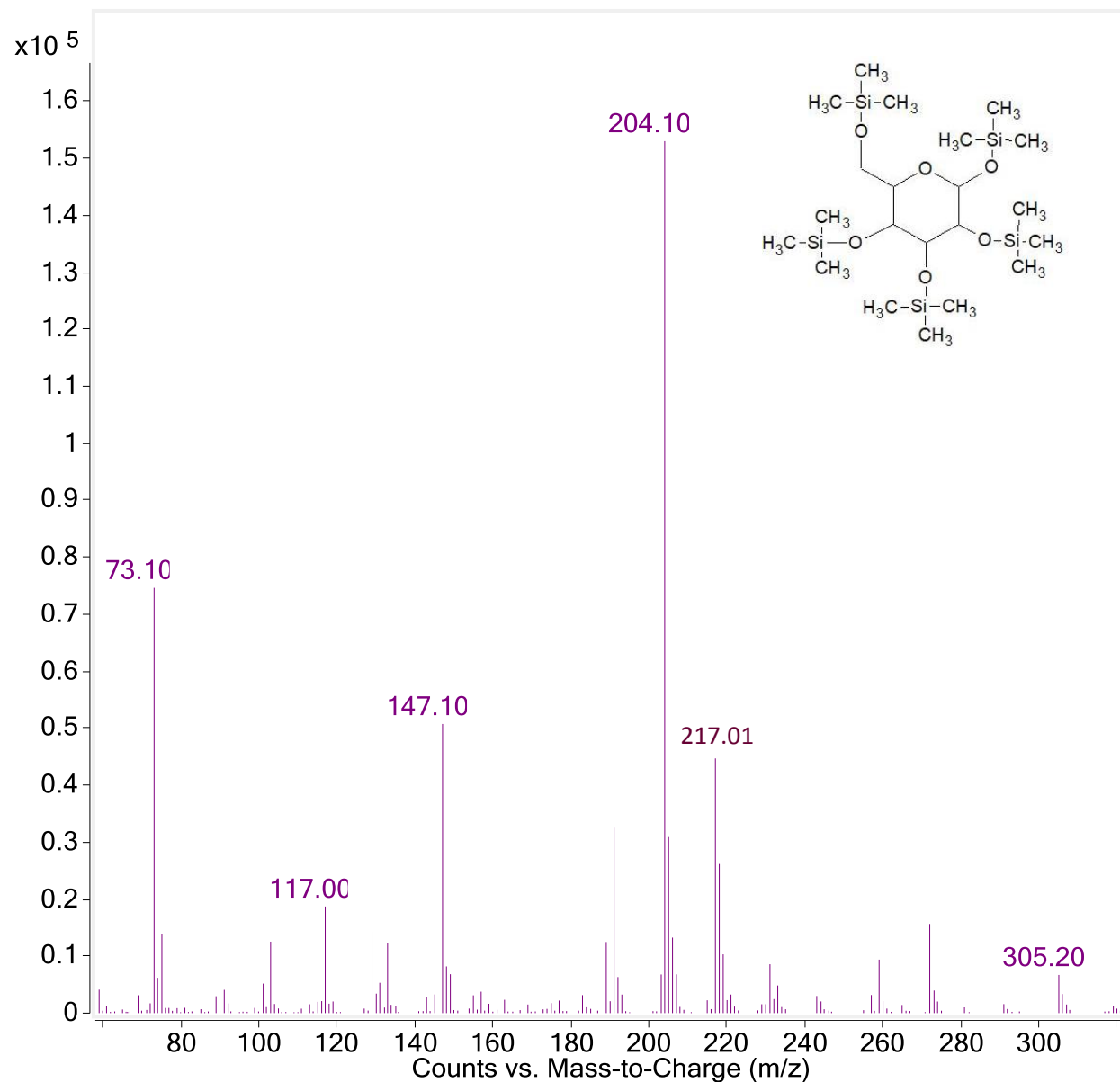


Figure 18. Mass spectrum and structure of penta(trimethyl)silylated [TMSi]-glucose. The spectrum was extracted from the TIC of glucose seen in Figure 17, which had a scan range of 48 to 800 m/z . Several high mass ions in the spectrum are formed by the loss of neutral fragments, typical of TMS derivatives. m/z 73, $(\text{CH}_3)_3\text{Si}^+$; m/z 117, $(\text{CH}_3)_3\text{SiOCH}_2\text{CH}_2^+$; m/z 147, $[(\text{CH}_3)_3\text{Si}^+]_2$; m/z 204, $[(\text{CH}_3)_3\text{Si}^+]_3$; lastly, m/z 305 $[(\text{CH}_3)_3\text{Si}]_4\text{CH}_2^+$. Although the molecular ion of 540 m/z was not observed.

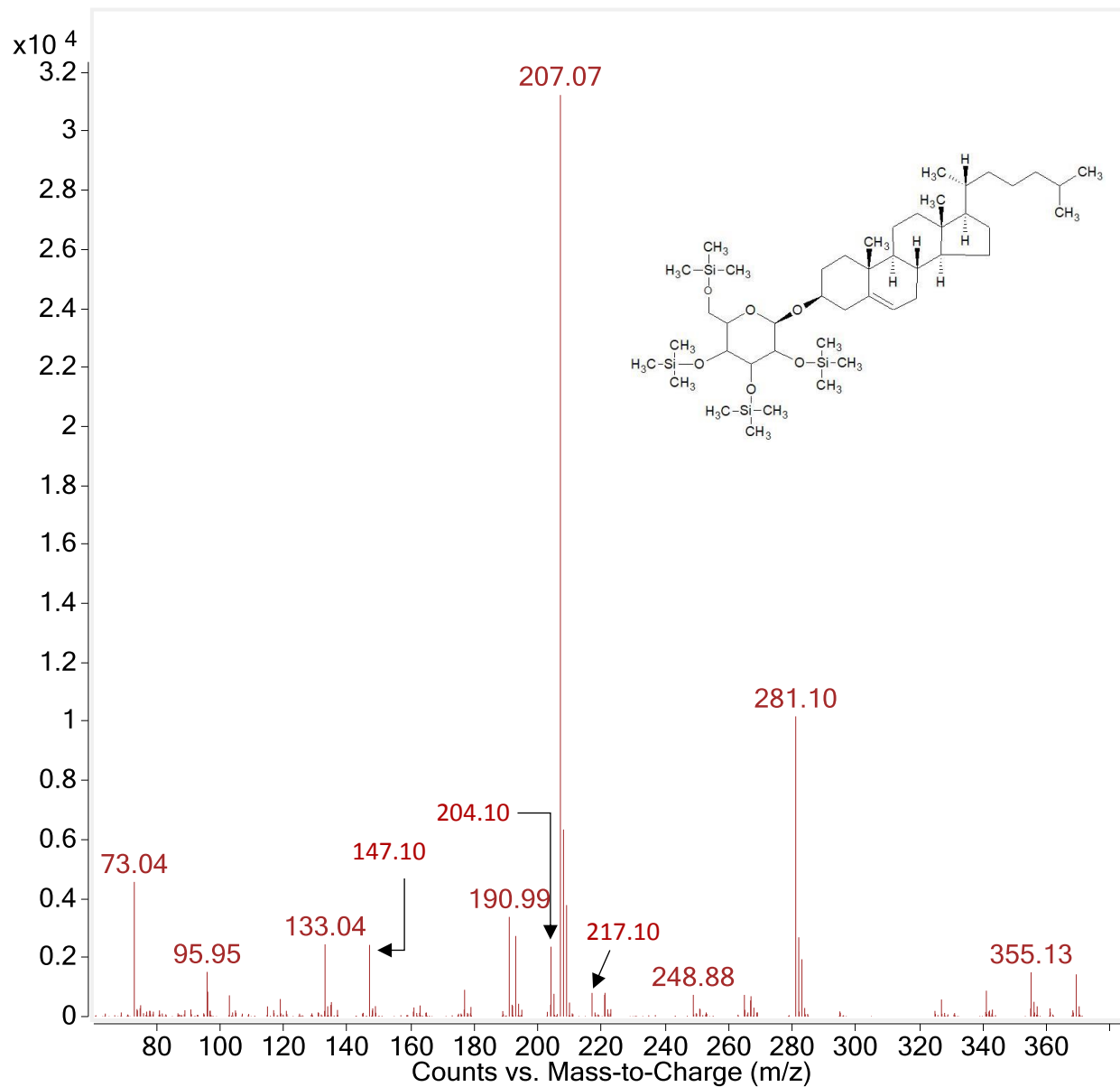


Figure 19. Mass spectrum and structure of tetra(trimethyl)silylated [TMSi] cholesterol glucoside. Characteristic ions of TMSi-glucose can be seen the mass spectrum, as described in Fig 18.

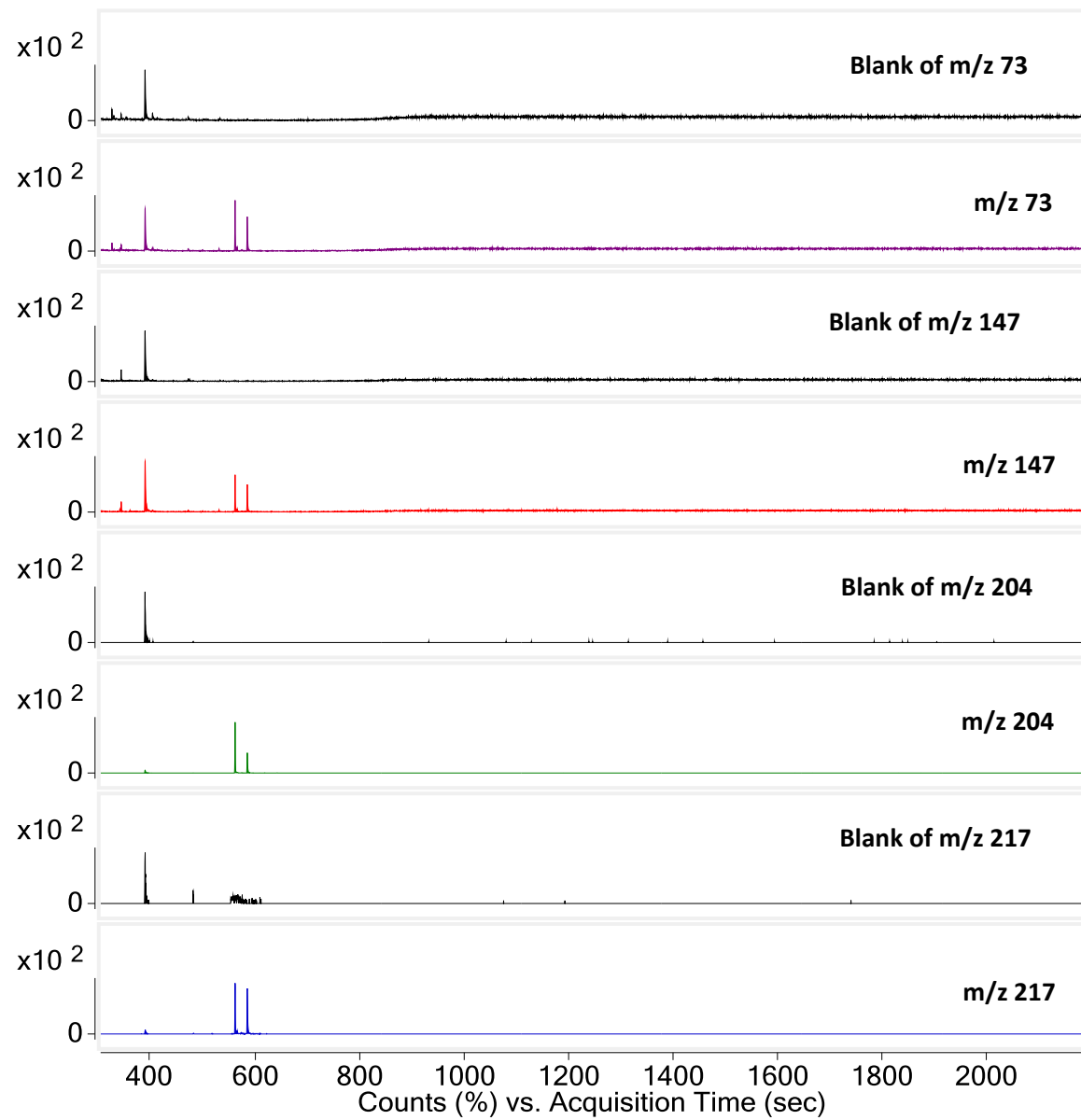


Figure 20. EIC of the 73 m/z, 147 m/z, and 204 m/z with their corresponding blanks as the top chromatogram. The retention time for each characteristic ion of TMSi-glucose all elute out in the same time window with the two distinct peaks seen in the TIC of glucose in figure 17 at 570 and 590 seconds.

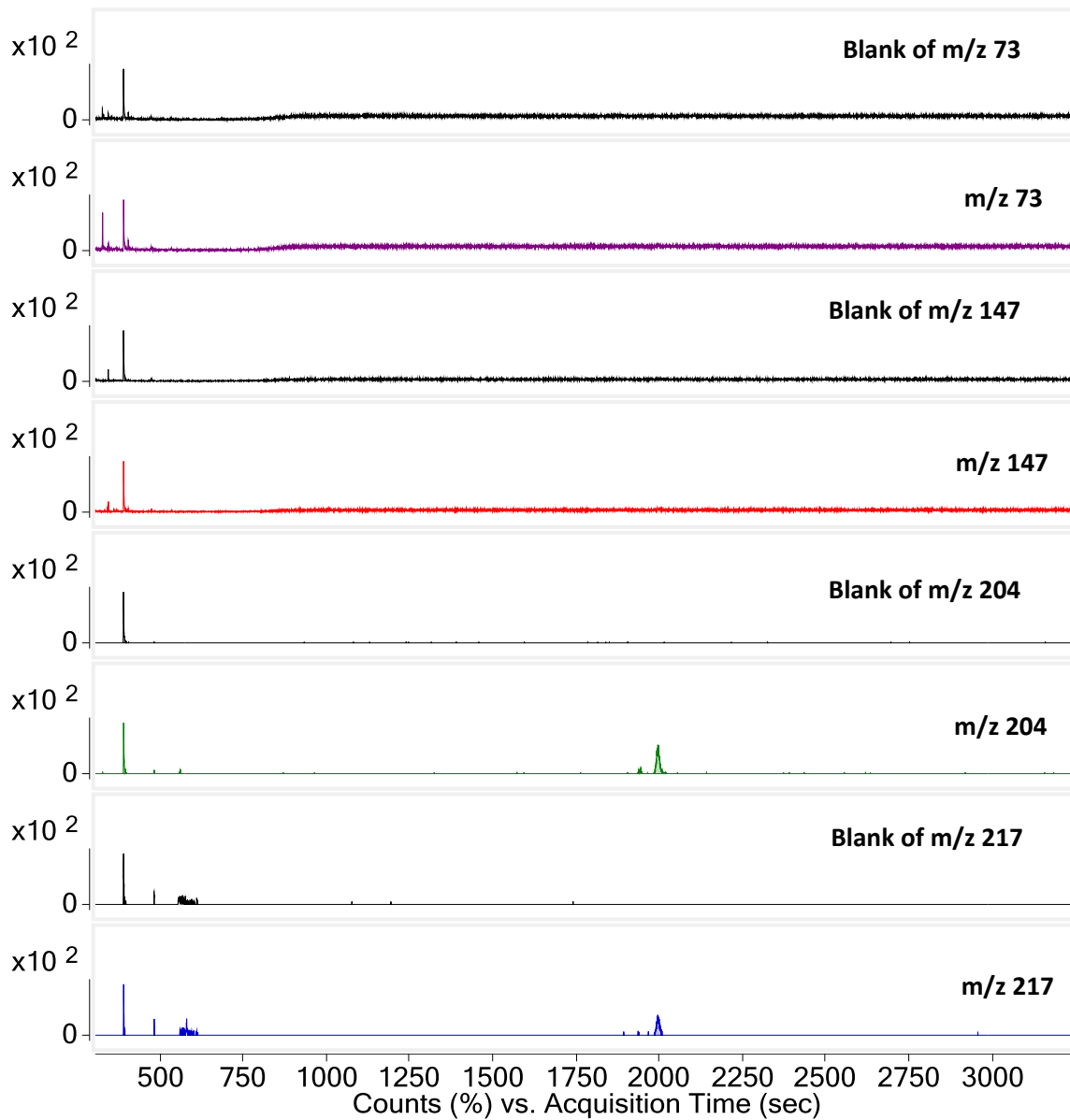


Figure 21. EIC of characteristic fragments of m/z 73, 147, 204, 217 from figure 17, at 2000 seconds.

3.4 Discussion

The analysis of the glucose and cholesterol glucoside standards, as their TMSi- derivatives, was performed using a GCMS with a 30-meter length high temperature capillary column with a thin film. Although this method enabled the separation of glucose from cholesterol glucoside, the TMSi-derivative of the mix SG standard did not elute out of the column, even though the column parameters were set to the maximum temperature recommend for column, which was a maximum holding time of 40 minutes at 325 °C. In contrast to other approaches, GCMS analysis with silylation of the SGs proved to be difficult due to the relatively low detection limit of cholesterol glucoside. The mass spectra data presented in Figure 19 for the TMSi derivative of cholesterol glucoside. The results for the TMSi derivative compared to those previously reported (Gutiérrez & del Río, 2001; Hoed, et al., 2008; Kovganko & Kashkan, 1999; Phillips , et al., 2004), neither the molecular ion or any other significant ions for the sterol moiety were observed above m/z 369. Furthermore, the lack of fragments especially the molecular ion produced from TMSi-cholesterol glucoside, made it challenging to distinguish between the target analyte and artefacts. In addition, the sample preparation by derivatisation with BSTFA was found to be labour intensive and time consuming. Thus, GCMS analysis with derivatisation using BSTFA was found to be inappropriate for the identification and quantification of the sterol glucoside.

Chapter 4 Acetylation of sterol glucosides for analysis by LC-MS/MS

4.1 Introduction

It is widely known that the sugar constituent of a sterol glucoside is generally glucose. Therefore, the SGs can be subjected to derivatisation. Derivatisation by silylation used in chapter 3, produced poor sensitivity for the TMS derivative of cholesterol glucoside. Furthermore, distinctive fragments reported for the sterol moiety of the SG were not observed with the glucoside fragments. Thus, characterising the SGs by the fragments was difficult. Acetylation is a form of a derivatisation reaction in which an acetic group is introduced to an organic compound (Conners & Pandit, 1978; Lepage, 1964; Licea-Perez, et al., 2016; Tiwari, et al., 2005). Typically, the hydroxyl group on the sugar moiety becomes an ester with the addition of the acetic group, as seen below in Figure 22. In this chapter, a simple and highly effective method is developed for the acetylation of SGs, in the aim of increasing the signal of SGs in the biodiesel, using the same LC-MS/MS instrument described from chapter 2.

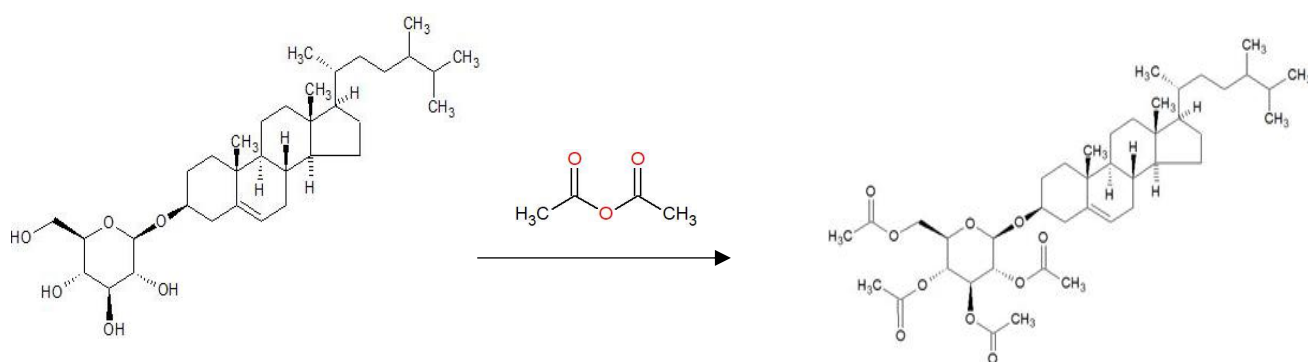


Figure 22. The acetylation reaction of campesterol glucoside with acetic anhydride.

4.2 Experimental

4.2.1 Materials

Samples of tallow-biodiesel and plant-biodiesel were acquired from Independent Petroleum Laboratory [IPL], located at Marsden Point, NZ. The biodiesel differed in appearance, of which one was clear liquid biodiesel, another was a dark yellow liquid biodiesel, two were of a pale liquid biodiesel, and one was of a dark brown liquid biodiesel, as seen below in Figure 23. As stated in previous chapters, soy-lecithin was bought from Countdown supermarket, located at Queen Street, AKL, NZ. Sterol glucoside [mix SGs] with a purity of >98% was obtained from Matreya, reported to contain 55% of sitosterol glucoside, 24.6% campesterol glucoside, 18% stigmasterol glucoside, and 1.4% avenasterol (Matreya LLC, 2018). Cholesterol glucoside standard (>97%), and all solvents used were obtained from Sigma Aldrich (Sigma-Aldrich, 2018)



Figure 23. Image of the biodiesel sample, analysed in this chapter. All were acquired from IPL.

4.2.2 Methods

4.2.2.1 Sample Preparation

Stock solutions for both samples and standards were prepared as follows; Lecithin, raw tallow, and biodiesel were each dissolved in MTBE to make a 10 g/L solution. A 5 g/L standard of mixed sterol glucoside and cholesterol glucoside were separately dissolved with methanol and chloroform (2:1 v/v). The biodiesel samples, lecithin and raw tallow were all diluted to a concentration of 100 µg/ml in 80% IPA. As mentioned in Chapter 3 and 4, all stock solution of the samples and standards were stored at -4 °C.

The preparation of standard curve are as follows; for standard A cholesterol glucoside and the mix sterol glucoside stocks were diluted to a concentration of 500 mg/L each in 80% IPA. From this, 500 µL was subsampled into a separate vial and made up to 1 mL using 80% IPA. This standard was serially diluted to yield 11 concentrations ranging from 500 mg/L to 0.488 mg/L. Each standard was then injected to LC-MS or subjected to the acetylation method, as described below, for LC-MS/MS.

4.2.2.2 Acetylation Procedure

20 µL aliquots of samples and standards were transferred to separate 1.8 mL amber glass vials. Afterwards, 40 µL of 1-methylimidazole and 400 µL of acetic anhydride was added and the mixture was vortexed. These were incubated at room temperature for 10 minutes. To stop the acetylation reaction, 500 µL of water (milli Q) was added and left to cool for another 10 minutes, before direct analysis by LC-MS/MS.

4.2.2.4 LC-MS/MS conditions

In this chapter, two methods are presented with different instrument parameters. Method A is a full scan LC-MS analysis of the acetylated SGs in positive mode, as seen in Table 11. Method B is LC-MS/MS analysis, as described in Table 12. The LC-MS/MS instrument remains as described in Chapter 2.

Table 11. Method A LC-MS conditions for full scan of acetylated SGs

Solvent A:	Acetonitrile with 0.1% Acetic acid		
Solvent B:	10% Acetonitrile, 10% Water, with added 10mM of concentrated Ammonia and 0.1% Acetic acid		
Solvent C:	80% Isopropanol, 20% Acetonitrile, 10mM of ammonia, and 0.1% acetic acid		
Source Parameters		Mass Spectrometer	
Gas temperature	300 °C	Scan range	580-800 m/z
Gas Flow	5 L/min	Scan time	500 seconds
Nebulizer	50 psi	Fragmentor voltage	110 V
Capillary voltage:	2000 V	Cell accelerator	7 V
V charging	1000 V	Polarity	Positive
Gradient Elution			
Time (minute)	% Solvent A	% Solvent B	% Solvent C
0.01	90.00	10.00	0.00
1.00	97.00	3.00	0.00
4.00	0.00	3.00	97.00
5.00	0.00	3.00	97.00
5.50	97.00	3.00	0.00
5.80	90.00	10.00	0.00

Table 12. Method B is LC-MS/MS conditions for MRM analysis of acetylated SGs

Solvent A:	Acetonitrile with 0.1% Acetic acid		
Solvent B:	10% Acetonitrile,90% Water, with added 10mM of concentrated Ammonia and 0.1% Acetic acid		
Solvent C	80% Isopropanol, 20% Acetonitrile, 10mM of concentrated Ammonia, and 0.1% Acetic acid		
Source Parameters			
Gas temperature:	300 °C		
Gas Flow:	6 L/min		
Nebulizer:	60 psi		
Capillary voltage:	2000 V		
V charging:	0 V		
Gradient Elution			
Time (minute)	% Solvent A	% Solvent B	% Solvent C
0.01	80.00	20.00	0.00
0.40	95.00	5.00	0.00
6.00	25.00	5.00	70.00
6.50	25.00	5.00	70.00
7.00	80.00	20.00	0.00

4.3 Results

Table 13 shows calculated m/z of common positive adducts of tetraacetylated derivatives of glucose and four sterol glucosides. We used these values to identify acetylated SG peaks in LC-MS data. Figure 25 shows the structural change to cholesterol glucoside from the acetylation reaction.

Table 13. Formula and calculated m/z of cations for tetraacetylated derivatives of glucose and four sterol glucosides.

compound	formula	tetra-acetylate formula	Derv MIM	Derv [M + H] ⁺	Derv [M + NH ₄] ⁺	Derv [M + Na] ⁺
glucose	C ₆ H ₁₂ O ₆	C ₁₆ H ₂₂ O ₁₁	390.16	391.16	408.19	413.15
cholesterol glucoside	C ₃₃ H ₅₆ O ₆	C ₄₁ H ₆₄ O ₁₀	716.48	717.48	734.52	739.47
sitosterol glucoside	C ₃₅ H ₆₀ O ₆	C ₄₃ H ₆₈ O ₁₀	744.51	745.51	762.55	767.50
stigmasterol glucoside	C ₃₅ H ₅₈ O ₆	C ₄₃ H ₆₆ O ₁₀	742.50	743.50	760.53	765.49
campesterol glucoside	C ₃₄ H ₅₈ O ₆	C ₄₂ H ₆₆ O ₁₀	730.50	731.50	748.53	753.49

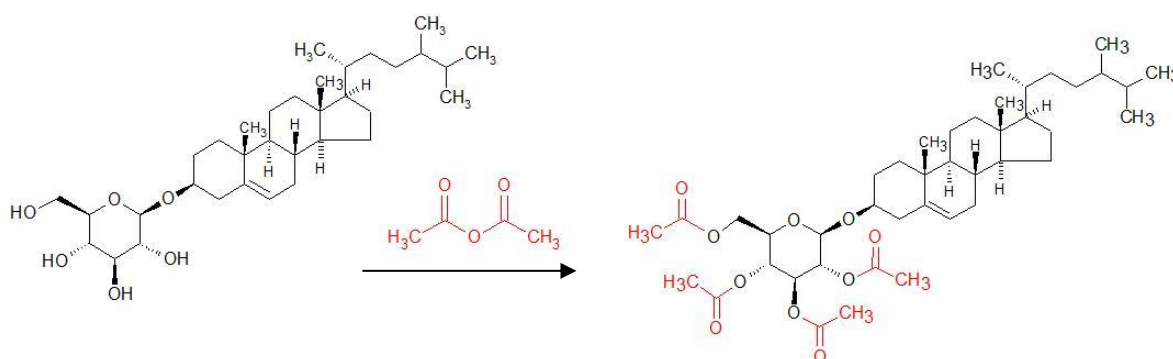


Figure 24. Derivatisation scheme for the reaction between campesterol glucoside and acetic anhydride in the presence of imidazole at room temperature

Figure 25, shows the mass spectra of the investigated derivatives obtained by LC-MS of the acetylated mixed SG standard. Interestingly, the mass spectrum of the acetylated SGs produced no signal for the protonated molecular ions [M + H]⁺. Instead, we observe an intense signal for ions with the m/z of 734.5, 760.6, 762.6, and 748.5, which corresponds with ammonium adducts of each

acetylated SG, shown in Table 14. The sodium adducts $[M + Na]^+$ can also be seen but at a much lower signal intensity. The mass spectra for acetylated campesterol glucoside shows ions of stigmasterol glucoside too, as they had co-eluted from the column.

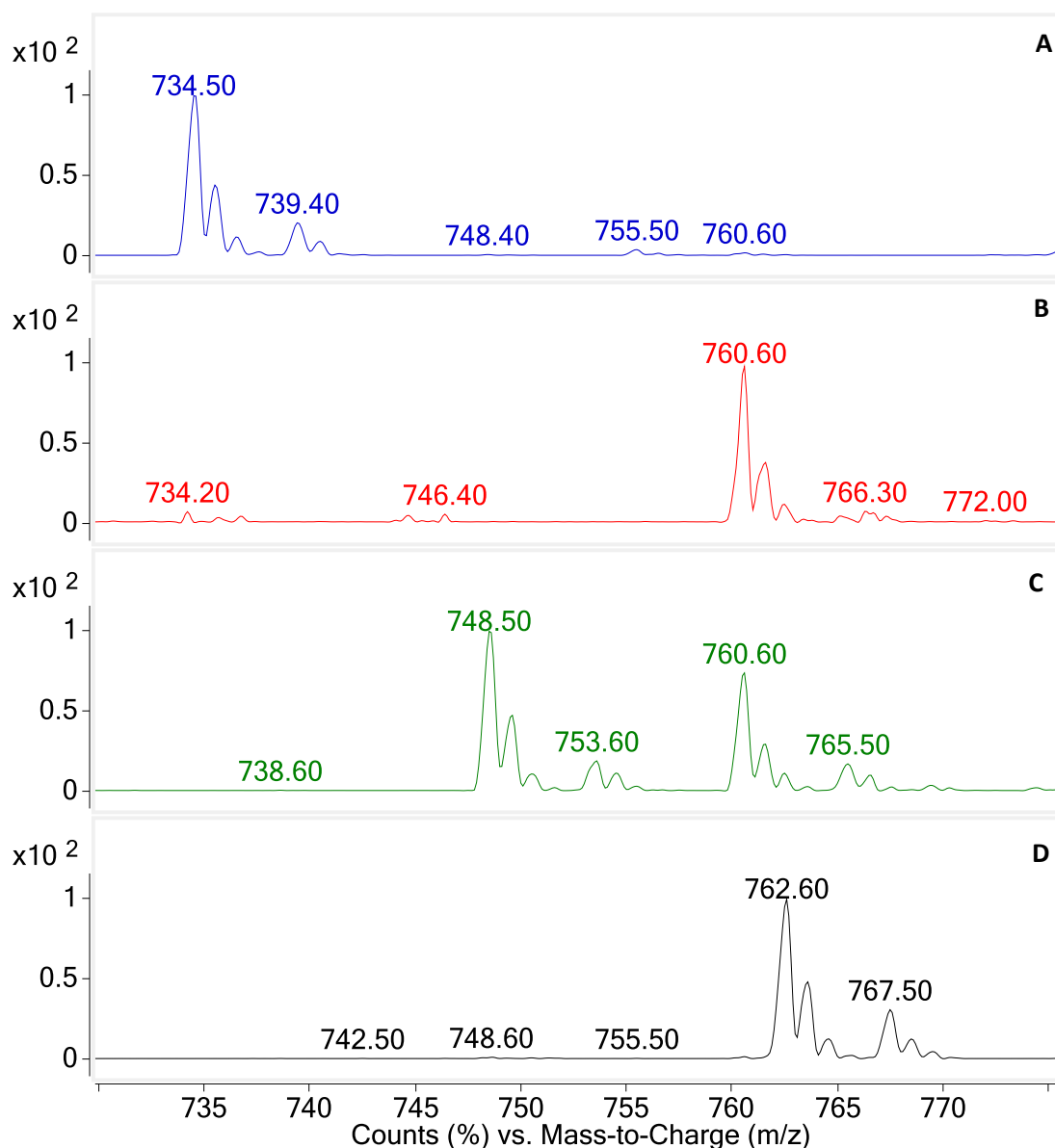


Figure 25. Mass spectra of each acetylated SG peak obtained from LC-MS of native sterol glucosides standards. (A) Cholesterol glucoside; (B) Stigmasterol glucoside; (C) Campesterol glucoside; (D) Sitosterol glucoside.

Figure 26 shows Extracted Ion Chromatograms for m/z of 608, 650, 692 and 734.5, which are the theoretical m/z of ammonium adducts of mono-, di-, tri- and tetra-acetylates of CholGluc. The only peak observed was for the tetraacetylate derivative. No peaks were observed corresponding to calculated m/z for any other positive ionisation adduct of these compounds (data not shown). From this we can conclude that the ten minutes allocated for the acetylation of the sterol glucoside is

sufficient to achieve complete acetylation of the four hydroxyl groups on the sugar moiety. The tetraacetylate of sterol glucosides appear to form abundant ammonium adducts, $[M + NH_4^+]^+$, under the ionisation conditions used.

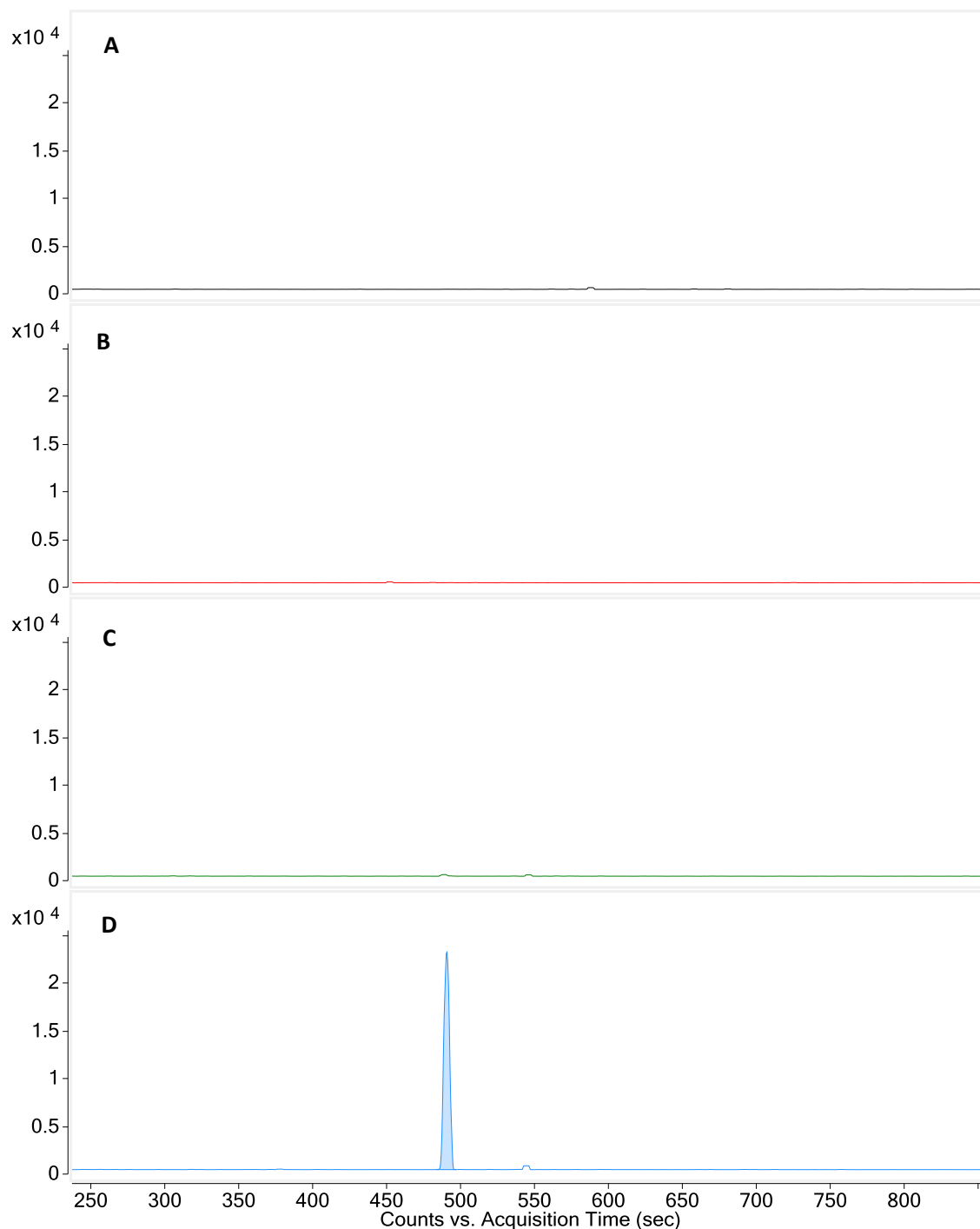


Figure 26. Extracted Ion Chromatograms illustrating complete acetylation of cholesterol glucoside. (A) m/z 608.5 corresponding to acetylation of one hydroxyl group; (B) m/z 650.5 for two hydroxyls; (C) m/z 692.5 for three acetylated hydroxyls; Lastly, (D) m/z 734.5 for all four hydroxyl groups being acetylated

Figure 27 shows fragmentation spectra obtained from Collision Induced Dissociation [CID] of SG acetylates. We observe base peaks of m/z 369, 383, 395, and 397, which are fragments corresponding to the sterol moiety of CholGluc, CaGluc, StGluc, and SiGluc, respectively. These ions are produced when the O-ether bond (O-C) between the sterol and sugar moiety is cleaved. In addition, we observe fragments of m/z 169, 271, and 331 in the mass spectra of ChloGluc, CaGluc, and SiGluc. For m/z 169, we suspect this fragment is produced by the ring break of the sugar moiety with two acetylate molecules. The fragment with $m/z \sim 331.1$ corresponds to the protonated ion of dehydrated glucose tetraacetylate $[M - \text{sterol} - \text{NH}_4 - \text{H}_2\text{O} + \text{H}^+]^+$. Dehydration probably occurs as a result of ether bond cleavage. Also seen in Figure 27, are the chemical structure of each acetylated SG, here the cleaving of the ether bond is indicated by a red dotted line. The optimised conditions for each acetylated SG, produced by Agilent Optimizer software, can be seen in Table 14.

Table 14. MS/MS parameters for multiple ion monitoring [MRM] for the investigated sterol glucoside derivatives in the positive ESI.

sterol glucosides	Precursor ion MS1 (m/z)	Product ion MS2 (m/z)	Dwell time (ms)	Fragmentor voltage (V)	Collision energy (eV)
cholesterol glucoside	734.5	369.4	250	185	15
campesterol glucoside	748.5	383.4	250	135	15
stigmasterol glucoside	760.5	395.1	250	150	14
sitosterol glucoside	762.5	397.4	250	140	19

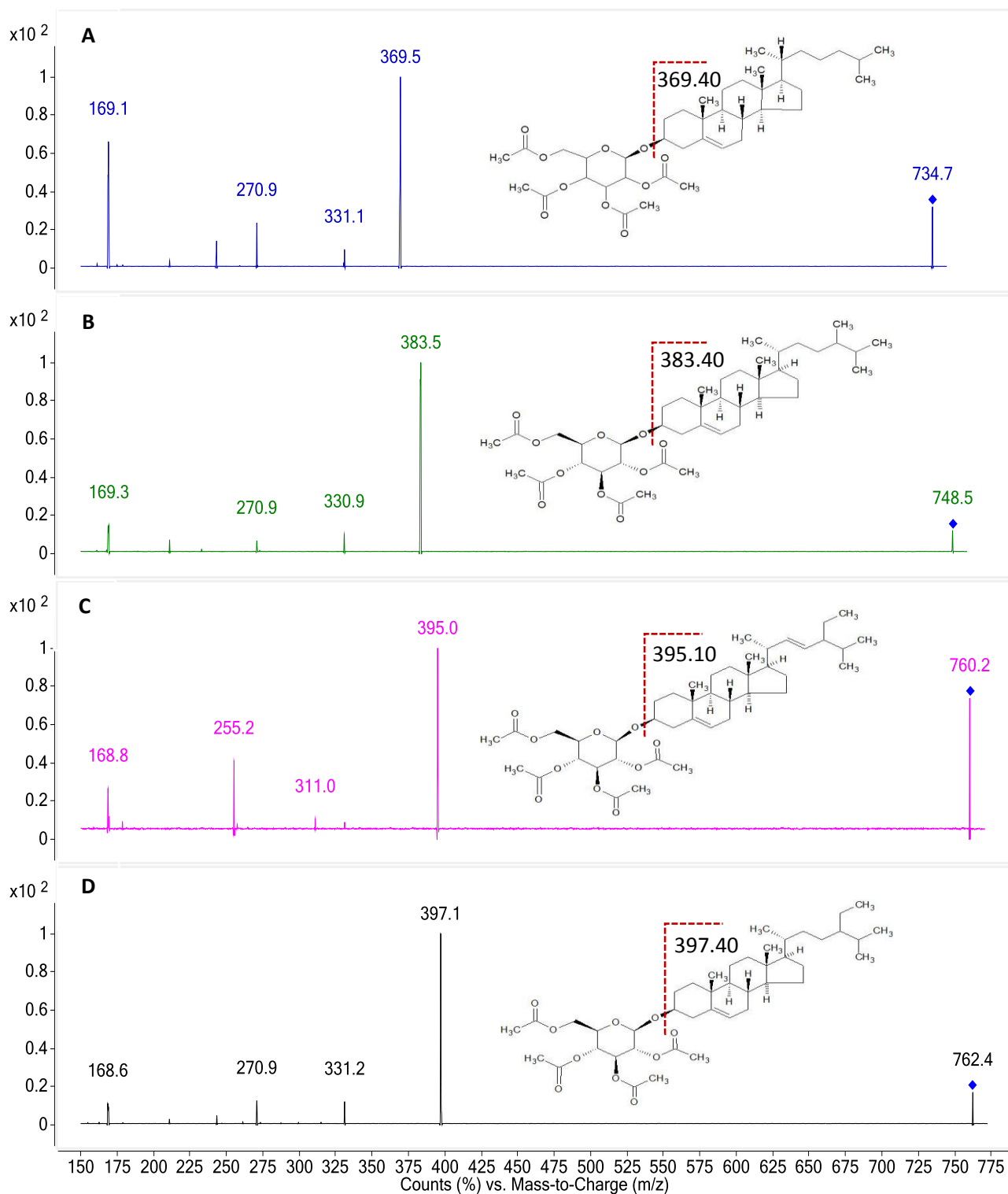


Figure 27. Product ion scans of the acetylated SGs, obtained using CID with collision energy at 15 V and fragmentor voltage at 135 V. (A) cholesterol glucoside, m/z 734.5; (B) campesterol glucoside, m/z 748.5; (C) stigmasterol glucoside, m/z 760.5; (D) sitosterol glucoside, m/z 762.5.

Figure 28 shows the three TIC chromatograms from LC-MS/MS analysis of acetylated CholGluc, mix SG standard, and lecithin. From the chromatogram, we can see the peaks in lecithin align with the peaks in of mix SGs, confirming the identity of the SGs in lecithin using retention time.

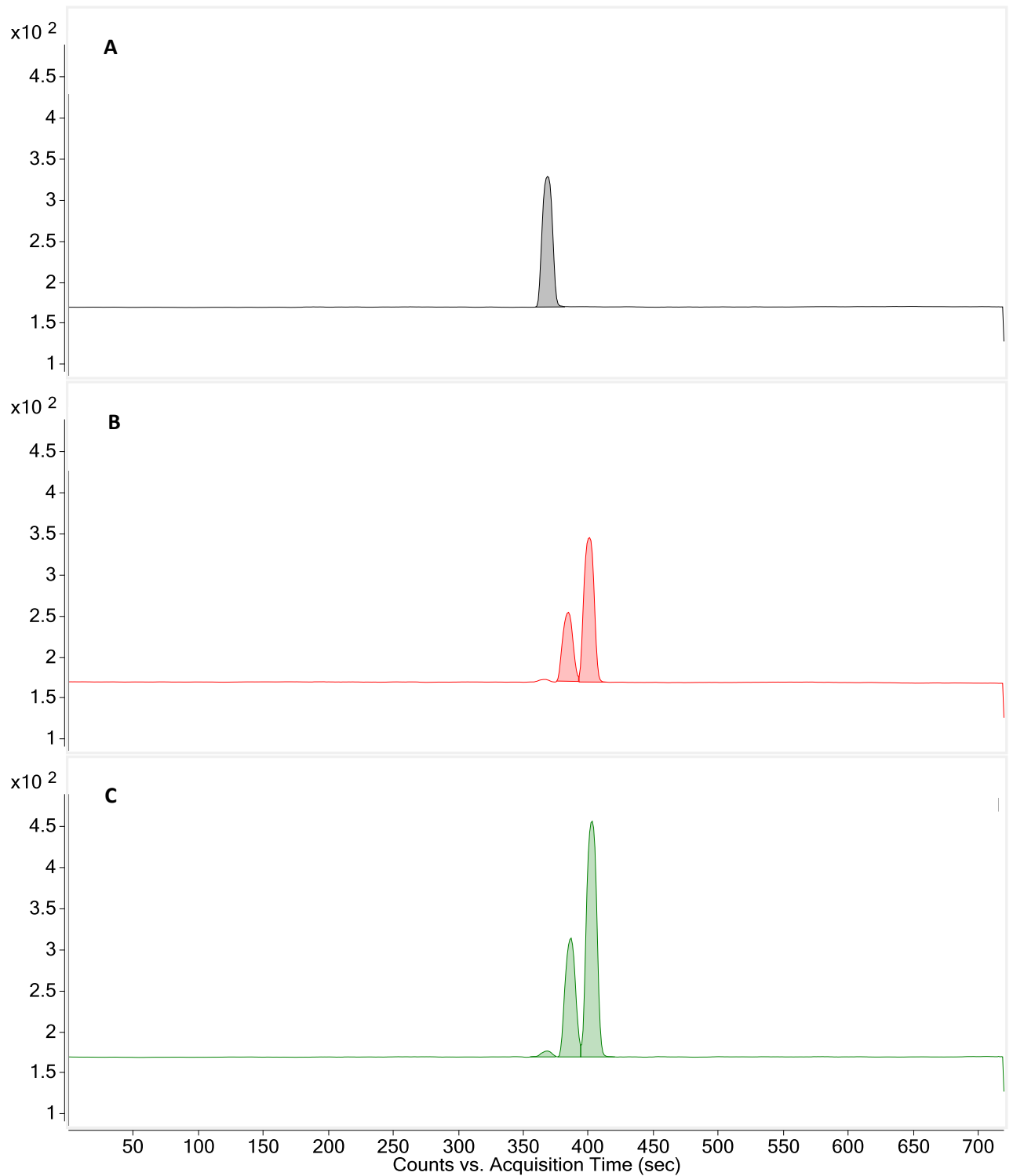


Figure 28. TIC chromatogram from LC-MS/MS of acetylated (A) cholesterol glucoside, (B) mix sterol glucoside standard, (C) Lecithin.

The calibration curve of cholesterol glucoside in Figure 29 showed an excellent linearity with a correlation coefficient of $r^2 > 0.999$ (Figure 29). The concentration of the standard ranged from 250 mg/L to 0.489 mg/L. The LOD and LOQ were measured to 0.129 mg/L and 0.429 mg/L, respectively. To account for the dilution factor [DF] of the acetylation procedure, MDL was estimated to be 21 mg/L.

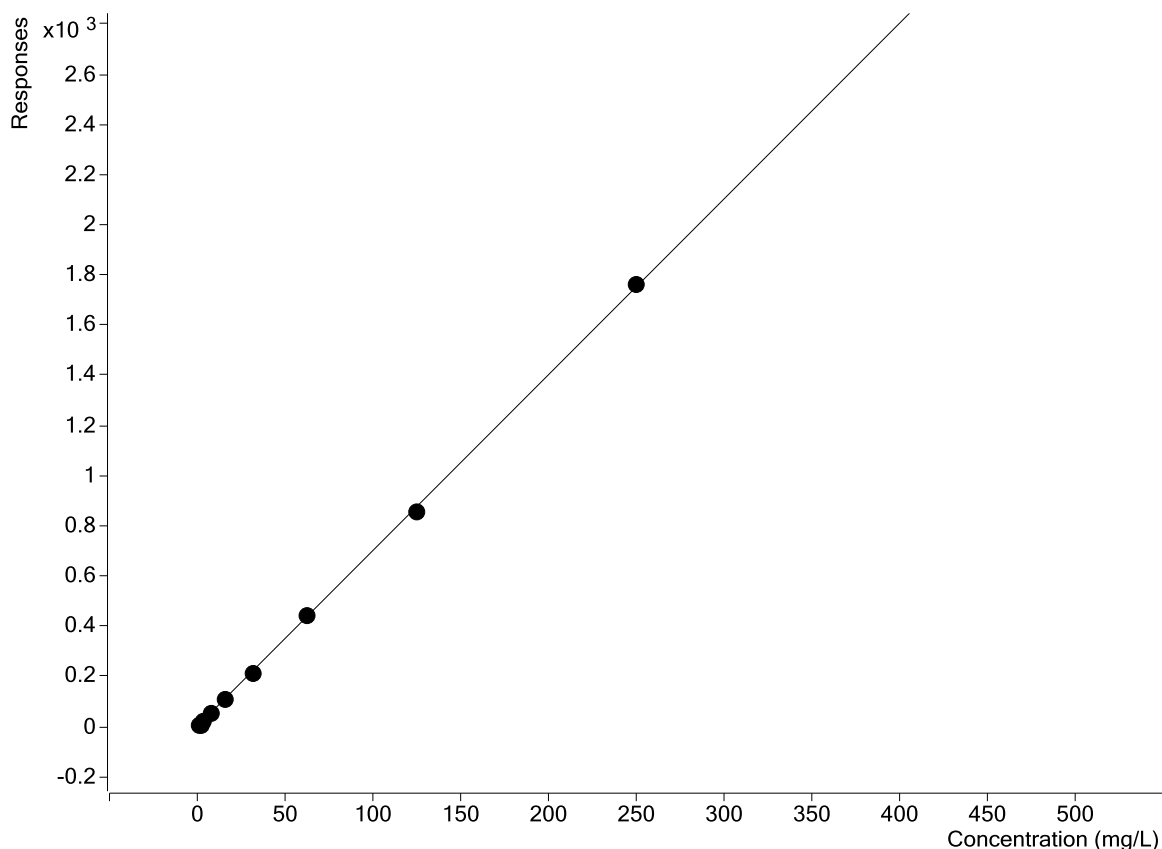


Figure 29. Standard curve for cholesterol glucoside tetraacetate. The concentration ranged from 250 to 0.488 mg/L, with an excellent linear regression, $r^2 > 0.999$ and $y = 7.008x$.

Although the LC-MS/MS method could now be used for identification of SGs in lecithin, when the acetylation and MRM method was applied to tallow-derived-biodiesel no peaks were observed and recovery of the internal standard was very low. Figure 30 shows MRM chromatograms for cholesterol glucoside tetraacetylate from a solvent blank, lecithin and plant-biodiesel A and B. Each had been spiked with 50 μ L of 500 mg/L cholGluc as internal standard. The peak in lecithin is only 8% of that in the blank, and for both biodiesel samples it was 3%.

The concentrations of different SGs in the mixed SG standard and in the lecithin was estimated using the standard curve of cholesterol glucoside, on the assumption that the response factor for all the sterol glucosides would be the same. However, due to the low recovery of the

internal standard the concentrations were impossibly high. The Matreya standard of SGs is declared to contain approximately 56% SiGluc, 25% CaGluc, 18% StGluc, and 1% avenasterol, by mass, although these proportions are stated to vary from batch-to-batch (Matreya LLC, 2018). On the assumption that the peak areas reflect the proportions of different SGs they indicate a ratio of 63% SiGluc, 30% CaGluc and 6%StGluc, quite different from the nominal values.

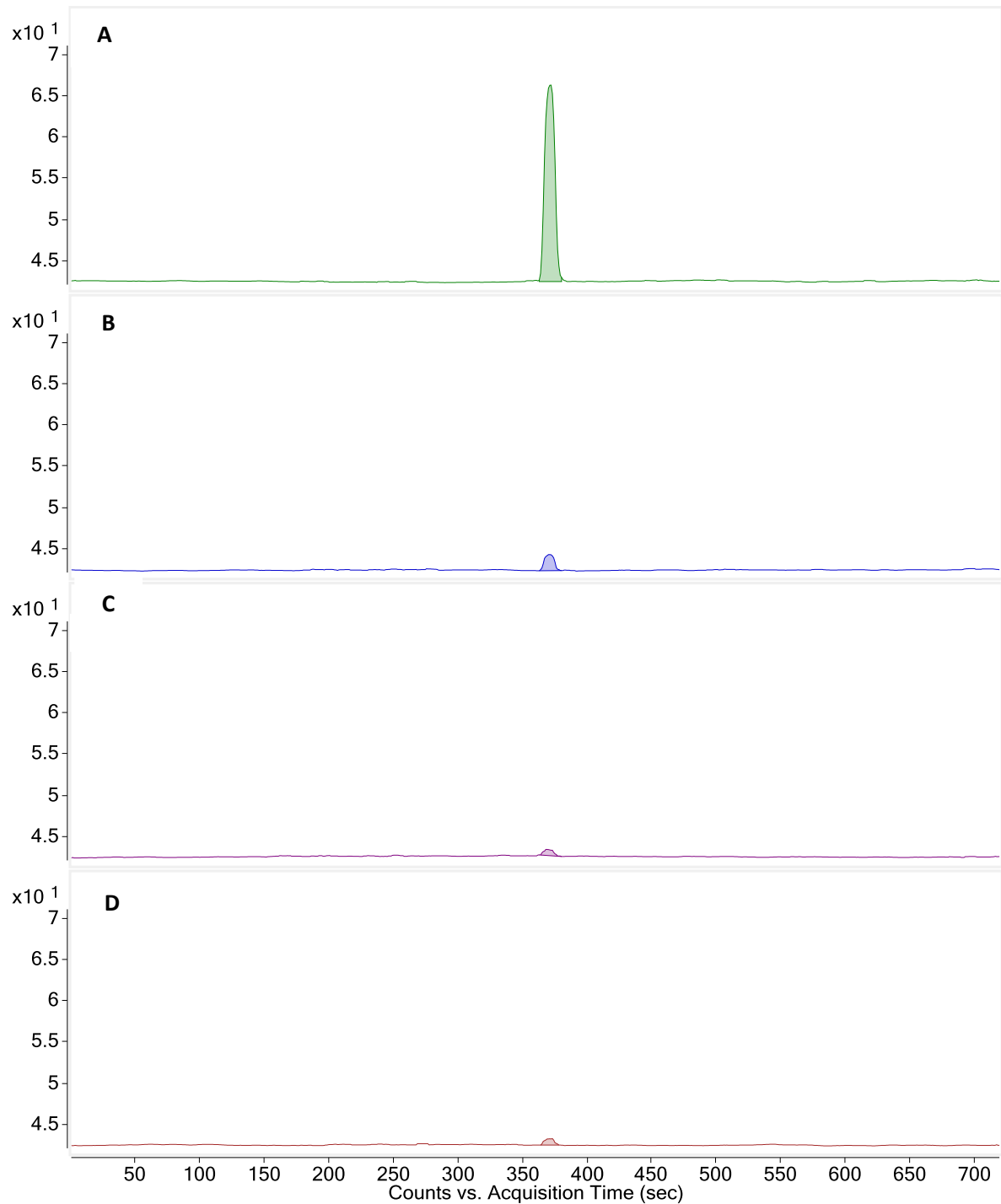


Figure 30. MRM chromatograms for cholesterol glucoside tetraacetate in a blank (A), lecithin (B) and two biodiesel samples (C) & (D). A 50 μ L volume of 500 mg/L cholesterol glucoside was spiked into each sample prior to acetylation.

4.4 Discussion

As sterol glucoside contains a sugar moiety with multiple hydroxyl functional groups, it was decided to investigate acetic anhydride as the derivatisation reagent in the hope that acetylation would make them more amenable to CID and MS/MS. Initially, the common method for acetylating the SGs were tried with acetic anhydride in the presence of pyridine, 4-dimethylaminopyridine [DMAP] was also investigated as a catalyst in the reaction. After several attempts using different temperatures that ranged from room temperature to 80 °C, including a time series from 10 minutes to 2 hrs, no signal of acetylated SGs were detected in the LC-MS/MS. With reports of methylimidazole being a superior catalyst than pyridine in the acetylation of hydroxyl groups (Connors & Pandit, 1978; Licea-Perez, et al., 2016; Tiwari, et al., 2005), methylimidazole was successfully applied for the acetylation of SGs. The acetylation procedure was optimized, where 20 µL of sample was mixed with 40 µL of methyl imidazole and 400 µL of acetic anhydride, after 10 minutes at room temperature, 500 µL of water was added to react with the excess acetic anhydride to stop the acetylation reaction. Monitoring the EICs of calculated m/z for potential semi-acetylate products confirmed the completion of the acetylation reaction. A single peak at m/z 734.5 was observed, indicating complete acetylation of the SGs in 10 minutes compared to 1hr required for the acetylation of sugars reported by Licea-Perez, et al., (2016).

The LC-MS/MS method developed here achieves the stated aim of developing a highly selective method for quantifying sitosterol glucoside, stigmasterol glucoside and campesterol glucoside. From the MRM scan, we observed a fourth peak eluting out in the StGluc MRM chromatogram, slightly before that peak. We suggest this peak is avenasterol glucoside as others have reported the presence of this isomer of StGluc and it is nominally present at trace amounts (~1%) in the mixed SG standard (Phillips, et al., 2005). Unfortunately, the response for this peak was below the limits of LOD of 0.129 mg/L. Therefore, we can only suggest that identity based on the precursor ion and product ion. Interestingly, there appeared to be a trace of CaGluc in the CholGluc standard as well. The purity of the CholGluc was reported to be >97% so this is plausible.

The concentrations of SGs calculated in the mixed SG standard were impossibly high. This could be because the response factor of the cholesterol glucoside standard is not representative of the other sterol glucosides, or that its behaviour as an internal standard is not representative. Due to the poor recovery of the internal standard we could not confirm this.

When tallow-biodiesel were analysed by acetylation and MRM, no peaks were observed. In published literature, there were no mentions of SGs in tallow. As such, plant-derived-biodiesel was also analysed, but the only peak observed was the internal standard. This was suspected that the

matrix of biodiesel may have inhibited the acetylation reaction. Therefore, in the next chapter we will address the matrix effects of plant-derived biodiesel upon the acetylation reaction.

Chapter 5 Trace Analysis of SGs in Plant based biodiesel

5.1 Introduction

Whereas cholesterol glucoside is the most abundant endogenous sterol glucoside in animal fat, campesterol-, stigmasterol-, and sitosterol-glucoside are the most frequently reported SGs in plants and plant-derived-biodiesel (Bondioli, et al., 2008; Gerpen, et al., 2011; Lascoste, et al., 2009; Moreau, et al., 2008; Songtawee, et al., 2014) . In this chapter, the two LC-MS methods presented in chapter 3 and 5 will be applied to biodiesel derived from plants. We continued to apply both full-scan LC-MS methods targeting native SGs and the acetylation method followed by LC-MS/MS in the hope that the former, simpler method would prove effective, complying with our aim of developing a relatively simple method. In case this did not prove possible we continued with the more complex but specific and sensitive LC-MS/MS method.

However, as the method detection limits had proven inadequate for detecting SGs in biodiesel it was necessary to develop a technique for removing the matrix effects from the abundance of fatty acid methyl esters [FAMES] in the biodiesel. These compounds comprise the majority of the biodiesel matrix and, due to their low polarity, it would be difficult to separate the SGs from them using conventional extraction techniques such as Solid Phase Extraction [SPE] or Liquid-Liquid Extraction [LLX]. Matrix effects are also the reason why the biodiesel had to be diluted 10,000 times for injection to LC-MS as the FAMES would have been retained on the LC-column and likely caused ion suppression as they eluted.

In order to eliminate the effects of the FAME matrix upon the LC-MS analysis, we saponified the biodiesel to convert the non-polar FAMES to more polar soaps. The non-saponifiable SGs could then be extracted from this polar matrix by LLX and the extraction injected straight to LC-MS. Not only should this approach increase the concentration of SGs being injected but it should also reduce matrix effects from the FAMES.

5.2 Experimental

5.2.1 Materials

Samples of plant-biodiesel were obtained from Independent Petroleum Laboratory [IPL], located at Marsden Point, NZ. Both samples are a brown liquid, shown in Figure 31. As stated in previous chapters, soy-lecithin was bought from Countdown supermarket, located at Queen Street, AKL, NZ. Sterol glucoside [mix SGs] with a purity of >98% was obtained from Matreya, reported to contain 55% of sitosterol glucoside, 24.6% campesterol glucoside, 18% stigmasterol glucoside, and 1.4% avenasterol (Matreya LLC, 2018). Cholesterol glucoside standard (>97%), and all solvents used were obtained from Sigma Aldrich (Sigma-Aldrich, 2018).

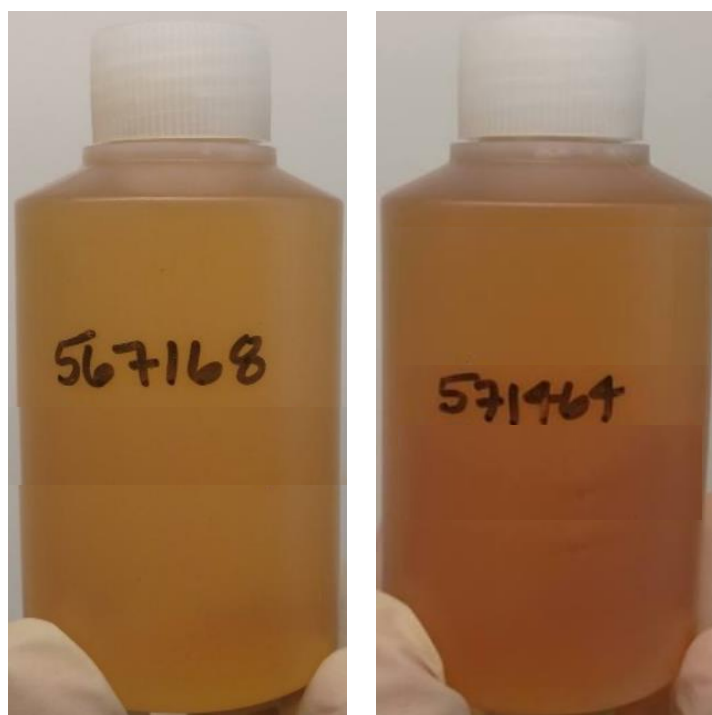


Figure 31. Plant based biodiesel acquired from Independent Petroleum Laboratory [IPL].

5.2.2 Analytical Columns

The LC-MS/MS instrument remained the same, as described in previous chapters except for the column. Two different columns were used in this chapter: a Poroshell 120 EC-C18 (2.1 x 50 mm, 2.7 μm) used in Method A, and a XSelect CSH C18 Column 130Å (2.1 mm X 100 mm, 3.5 μm) for Method B.

5.2.3 Methods

5.2.3.1 Biodiesel Saponification Procedure

Approximately 5 mg of biodiesel was dispensed into a vial and the mass recorded to ± 0.1 mg. A 50 μL volume of 500 mg/L cholesterol glucoside and 2 mL of 1M ethanolic potassium hydroxide [KOH] was added to each vial and they were left to reflux on a heating block for 2 hours at 90 °C. 4 mL of water was added to stop the reaction. The saponified samples were extracted using 6 mL of a non-miscible solvent, either dichloromethane [DCM] or Ethyl Acetate [EtAc]. To increase the concentration of the SGs, the solvent was evaporated using a centrifugal concentrator and the dry residue redissolved in 800 μL of EtAc and acetone (3:1 v/v). This extract was either injected straight to LC-MS or used for acetylation, as described in chapter 5, before injection to LC-MS/MS.

5.2.3.2 Determination of matrix effects using saponification

Four different masses of biodiesel were weighed into separate vials prior to saponification described above. The masses were 20 mg, 10 mg, 5 mg, and 2 mg. Each sample was then spiked with 50 μL of 500 mg/L cholesterol glucoside standard before continuing with the saponification and acetylation procedure. Matrix effects were monitored by the Response Factor [RF] of the internal standards of cholesterol glucoside and mixed SGs in the spiked samples.

5.2.3.2.3 LC-MS/MS Conditions

Method A, using full scan LC-MS with multimode ionisation [MMI] was carried out on an Agilent Poroshell 120 EC-C18 (2.1 x 50 mm, 2.7 μm) column. The MMI source conditions are listed in Table 15.

Table 15. Method A LC-MS conditions in Negative mode

Solvent B:	Acetonitrile with 0.1% Acetic acid
Solvent C:	10% Acetonitrile, 90% Water, 10mM ammonia and 0.1% acetic acid
Solvent D:	80% Isopropanol, 20% Acetonitrile, 10mM ammonia and 0.1% acetic acid
Source Parameter	
Gas Temperature	300 °C
APCI Heater	200 °C
Gas Flow	5 L/min
Nebulizer	50 psi
Capillary	2000 V
Charging voltage	500 V
APCI Needle Negative	4

Table 15. Continued

Scan range		m/z 580 to 645		
Gradient Elution				
Time (minute)	% Solvent B	% Solvent C	% Solvent D	
0.01	80.00	20.00	0.00	
0.40	80.00	20.00	0.00	
6.00	30.00	10.00	60.00	
6.80	90.00	10.00	00.0	
7.50	80.00	20.00	0.00	

The final optimized condition for MRM analysis was conducted on an XSelect CSH C18 Column 130Å (4.6 mm X 100 mm, 3.5 µm), using conditions described in Method B, seen here in Table 17. The initial injection volume was 5 µL.

Table 16. Method B LC-MS/MS conditions for ESI-MRM scan in positive mode.

Solvent B:	Acetonitrile with 0.1% Acetic acid				
Solvent C:	10% Acetonitrile, 90% Water, 10mM ammonia and 0.1% acetic acid				
Solvent D:	80% Isopropanol, 20% Acetonitrile, 10mM ammonia and 0.1% acetic acid				
Source Parameter					
Gas Temperature	300 °C				
APCI Heater	200 °C				
Gas Flow	6 L/min				
Nebulizer	60 psi				
Capillary	2000 V				
Gradient Elution					
Time (minute)	% solvent B	% solvent C	% solvent D		
0.01	40.00	60.00	0.00		
1.00	65.00	5.00	30.00		
6.00	35.00	5.00	60.00		
6.50	25.00	5.00	70.0		
7.00	40.00	60.00	0.00		
analyte	precursor ion (m/z)	product ion (m/z)	dwel time (ms)	fragmentor voltage (V)	cone voltage (V)
cholesterol glucoside	734.5	369.4	250	185	15
campesterol glucoside	748.5	383.4	250	135	15
stigmasterol glucoside	760.5	395.1	250	150	14
sitosterol glucoside	762.5	397.4	250	140	19

5.3 Results

5.3.1 LC-MS of saponified, extracted sterol glucosides

No SGs besides the internal standard were observed in the LC-MS analysis of saponified, extracted biodiesel. The peak area of the internal standard after extraction with dichloromethane was negatively influenced by the mass of biodiesel, as shown in Figure 32. EtAc did not show any negative relationship and so we proceeded with ethyl acetate as extraction solvent.

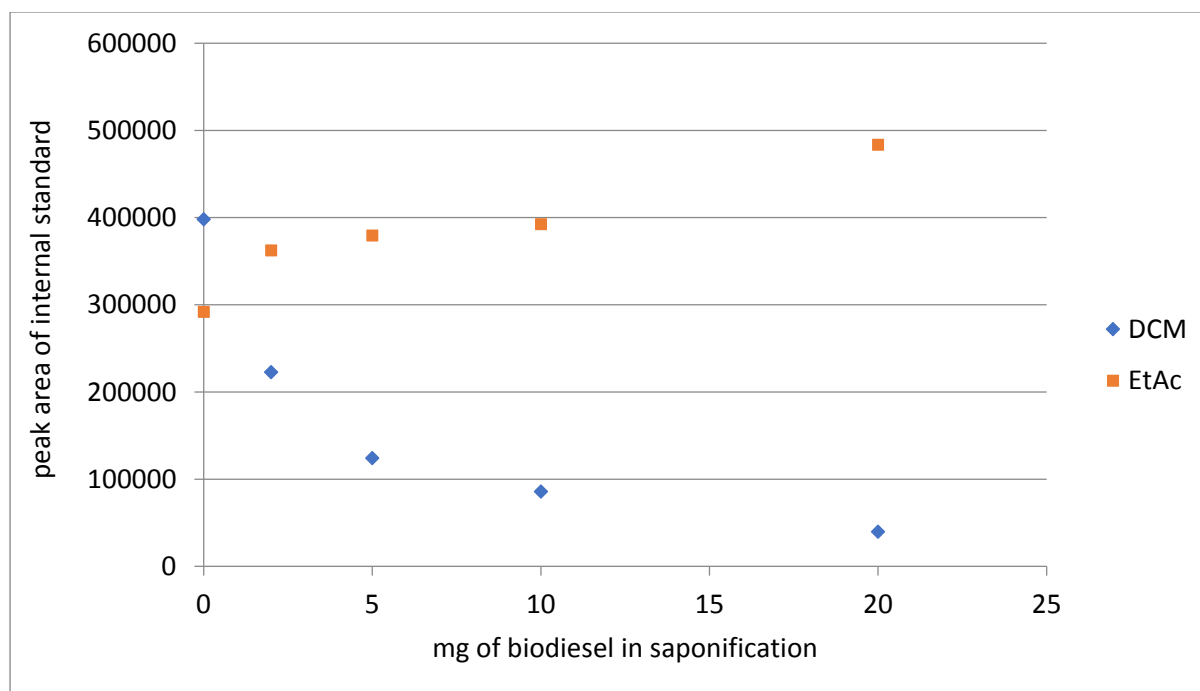


Figure 32. Effect of different masses of biodiesel upon peak area of the internal standard.

The calibration curve obtained from the LC-MS analysis was linear with an $r^2 > 0.995$. The LOD, and LOQ for these injections were calculated to be 0.25 and 0.85 mg/L, respectively. These values are improvements over previously reported LOD of 30 ppm and 100 ppm, by >100-fold, using GC and HPLC methods (Montpetit & Tremblay, 2016; Moreau, et al., 2008). However, once the overall dilution factor of 48 times is taken into account the overall Method Detection Limit [MDL] on multiplying the LOQ by the dilution factor of 48, produced the value of 40.8 mg/L.

Matrix effects [ME] were evaluated for the acetylation reaction due to the low recovery of internal standard. Assessing ME was accomplished by monitoring the Response Factor [RF] of cholesterol glucoside spiked onto different masses of biodiesel prior to saponification, extraction and acetylation. Table 17 displays the calculated RF for each diluted sample. Interestingly, we can observe that as the sample mass decreases, the RF increases. In fact, the RF for 2 mg was greater by >30-fold compared to the RF produced from 20 mg of biodiesel. From the data we can estimate the

mass required to achieve complete elimination of ME. However, this appeared to require vanishingly small masses of biodiesel. We decided to proceed with a mass of 5 mg biodiesel as below this value the accuracy of the balance (± 0.1 mg) would have started to affect our analysis and some matrix effects can be controlled for using the internal standard.

Table 17. The investigation of Matrix Effect by response factor, and comparison of solvent extraction.

DCM		EtAc	
Mass (mg)	Response factor (area/mg)	Mass (mg)	Response factor (area/mg)
20	5	20	12
10	16	10	46
5	47	5	144
2	169	2	335

5.3.1 LC-MS/MS of extracted, and acetylated sterol glucosides

For acetylated cholesterol glucoside, the calibration curve obtained from LC-MS/MS, had an excellent correlation coefficient of $r^2 > 0.9997$. The LOD and LOQ were 0.025 and 0.084 mg/L, respectively. Incorporating the dilution factor of 1920 mg/L, the MDL was estimated to be 161.28 mg/L. The XSelect CSH C18 Column was used to improve the resolution of SGs. In addition, the total analysis time of the SGs were improved from 17min to 12min compared to the Poroshell 120 C18 column used in chapter 2 and 4.

Very small peaks for acetylated sitosterol glucoside were evident in the two biodiesel samples for 5 μ L injections (data not shown). To increase the peak area the samples were reanalysed with an injection volume of 80 μ L, yielding quantifiable peaks for acetylated campesterol- and sitosterol-glucoside. Peaks for acetylated stigmasterol glucoside were evident but below the Limit of Detection.

Recovery of the internal standard was consistently high, with values of 187% and 197% for the two biodiesel samples and 166% for the lecithin. All of the acetylated SGs were quantified using the calibration curve of cholesterol glucoside and normalised to recovery of the internal standard. Table 18 shows the measured concentration of SGs found in the plant-based-biodiesel. From the table were able to measure all three SGs in the biodiesel. In 567168, we measured 20 ng/ μ g for CaGluc, 87 ng/ μ g StGluc, and 154 ng/ μ g for StGluc. For 571464, the concentration of SGs were 28 ng/ μ g of CaGluc, 3 ng/ μ g StGluc, and 55 ng/ μ g of SiGluc.

Table 18. The concentration of SGs measured in biodiesel.

	campesterol glucoside (µg/g)	stigmasterol glucoside (µg/g)	sitosterol glucoside (µg/g)
567168	84	<LOQ	149
571464	24	<LOQ	47

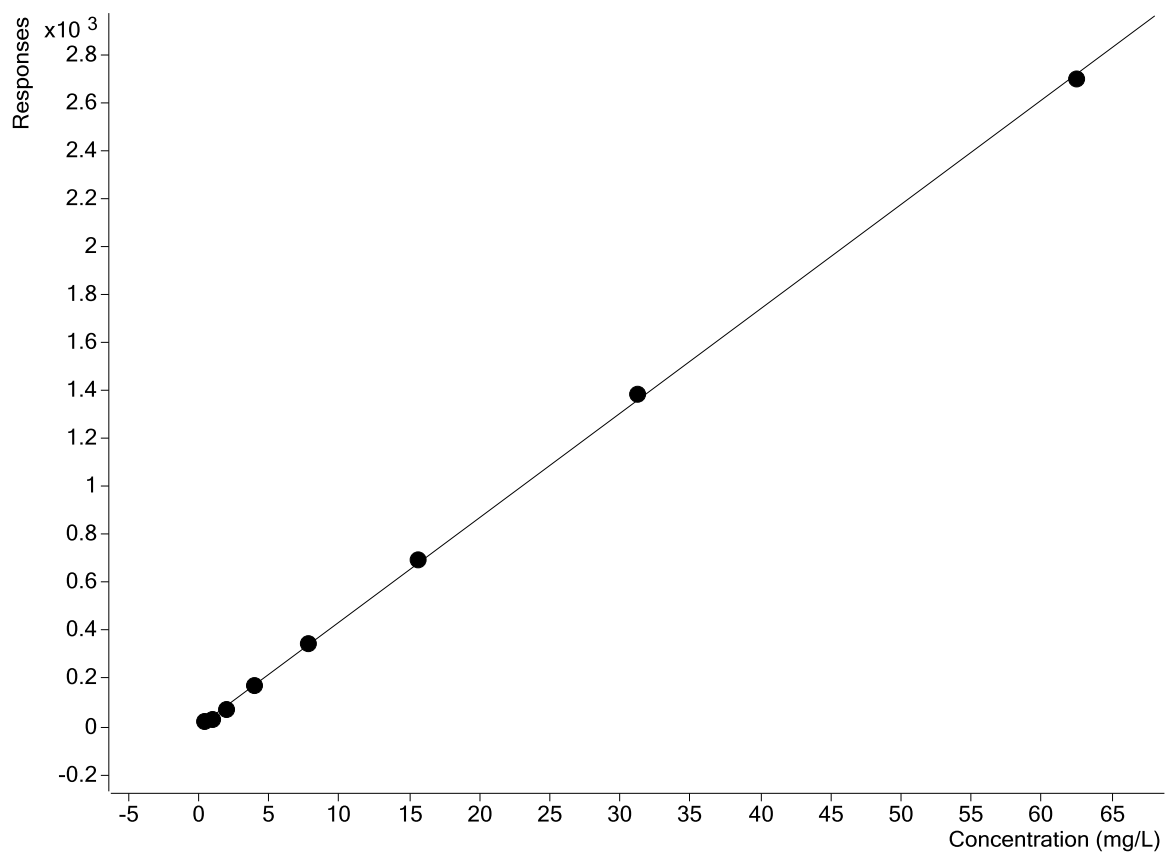


Figure 33. Calibration curve of cholesterol glucoside tetraacetate with a range of 62.5 mg/L to 0.488 mg/L. With a liner relationship, $y= 43.50x$, and $r^2 = 0.9997$.

5.4 Discussion

5.4.1 Matrix effect

When the SG content in the biodiesel were extracted and acetylated, there was no internal standard recovered after LC-MS/MS. This raised the concern that the stoichiometry involved in the saponification of the FAMES was hindered due to the amount of material being saponified, original mass of biodiesel was 100 mg. Therefore, the matrix effect for our sample was assessed by performing a series of dilutions by reducing the sample size to 20 mg, 15 mg, 10 mg, 5 mg, and 2 mg. The calculated RF of the cholesterol glucoside and the peak area were used to monitor the matrix effect. As expected, the more diluted the samples, the great the response, with 2 and 5 mg producing a RF of 335 and 144, respectively, as well as a peak area of around 3800 to 4000. EtAc was determined to be the superior solvent for extracting the SG as no negative relationship was observed.

5.4.2 LC-MS of saponified, extracted, and acetylated sterol glucosides

Once matrix effect was reduced by saponifying of the FAMES in the biodiesel, full scan analysis from chapter 3 was applied in the hope that the former simpler method would prove effective, complying with our aim of developing a relatively simple method. Although the MDL was significantly improved over chapter 3 from 234071 down to 40.8 mg/L, this was still too high as the threshold for total contaminants in the biodiesel is 24 mg/L. Therefore, we pursued a more complex but specific method by acetylating the saponified extract. In Table 19 the acetylated by LC-MS/MS produced the greatest sensitivity for the LOD and LOQ, 0.025 mg/L and 0.084 mg/L, respectively. However, due to the reduction of material and serial dilution from the saponification and acetylation procedure, the sensitivity of MDL is affected greatly by decreasing the sensitivity to 161.2 mg/L. To overcome this we increased the LC-MS/MS injection volume to 80 μ L, an increase of 16-fold, with a concomitant reduction in the MDL to 10.1 mg/L. However, this is poor chromatographic practice as such large injections can lead to chromatographic issues and increased matrix effects. Although no such artifacts were observed these results should be considered provisional. It would be simple to reproduce the analysis with matched standard and sample volume injections however the opportunity was not available to due time restrictions.

With consideration to the matrix effect, the total SGs in biodiesel were successfully quantified of the SGs in the fuels. As mention previously, the measured SGs in sample 567168, consisted of 84 ng/ug CaGluc, and 149 ng/ug for SiGluc. For sample 571464, the concentration of SGs were 24 ng/ug of CaGluc and 47 ng/ug of SiGluc.

Table 19. Summary of the limits of method presented in this thesis

	LOD (mg/L)	LOQ (mg/L)	MDL (mg/L)	r²
Native SGs LC-MS	7	23	234071	0.9957
Acetylated LC-MRM	0.129	0.429	21	0.9998
Saponified, acetylated SGs LC-MS	0.25	0.85	40.8	0.9954
Saponified, acetylated SGs LC-MS/MS (5 µL injection)	0.025	0.084	161.2	0.9997
Saponified, acetylated SGs LC-MS/MS (80 µL injection)	0.002	0.005	10.1	0.9997

Chapter 6 Summary and recommendation

6.1 summary

This study describes a highly selective LC-MS/MS method to detect campesterol glucoside, stigmasterol glucoside and sitosterol glucoside in biodiesel. Unfortunately, due to the occurrence of the matrix effect, the sensitivity of the final method was not especially sensitive or simple, although we did manage to achieve an MDL of 10.1 mg/L. The elimination of the matrix effect is an important aspect of SG analysis in biodiesel that required extensive method development and validation. In this study we have shown a variety of methods required to reduce the matrix effect and improve sensitivity and specificity of the analysis for the target compounds through the use of acetylation, saponification and liquid-liquid extraction.

We have measured concentrations of SGs in plant-based-biodiesel that exceed the total contamination criteria of 24 mg/kg, specified in EN 12662. As it has been reported that biodiesels that exceed this criteria can result in fuel filter blocking it is essential that accurate and sensitive methods such as the one reported here are available to measure those concentrations to allow the potential of these renewable fuel sources to be achieved.

6.2 Recommendations

In regards to this thesis, there are some components that need further investigating. For example, a more in-depth analysis is required to determine the significant influence of matrix effect in biodiesel. This can progress to improving sensitivity of detecting sterol glucoside and other trace contaminants in biodiesel. Once matrix effects have been minimised, the final methodology developed in this study could extend to routine analysis of the sterol glucoside and acetylated sterol glucoside content in the different biodiesel feedstock, as it is known that the composition of the oils affects the quality of biodiesel. This research can be further improved by the use pure standards of the target compounds for quantification as the use of cholesterol glucoside as a surrogate is sub-optimal. However, it was a pragmatic choice within the scope and budget of an MSc project.

References

- Agarwal, A. K., Gupta, T. & Kothari, A., 2011. Particulate emissions from biodiesel vs diesel fuelled compression ignition engine. *Renewable and Sustainable Energy Reviews*, 15(6), pp. 3278-8300.
- Banerjee, S. & Mazumdar, S., 2012. Electrospray Ionization Mass Spectrometry: A Technique to Access the Information beyond the Molecular Weight of the Analyte. *International Journal of Analytical Chemistry*, Volume 2012, pp. 1-40.
- Bondioli, P., Cortesi, N. & Mariani, C., 2008. Identification and quantification of setryl glucosides in biodiesel. *European Journal of Lipid Science and Technology*, 110(2), pp. 120-126.
- Borgman, D., 2007. *Agriculture, bio-fuels and striving for greater energy independence*. [Online] Available at: <https://www.wesrch.com/energy/paper-details/pdf-TR10VJ7K3WODA-agriculture-bio-fuels-and-striving-for-greater-energy-independence#page5> [Accessed 6 March 2018].
- Bradley, G., 2014. *Z energy plans 21m biodiesel plant*, Auckland: NZ Herald.
- Braus, H., ECK, J. W., Mueller, W. M. & Miller, F. D., 1957. Isolation and Identification of a Sterol. *Journal of Agricultural and Food Chemistry*, 5(6), pp. 458-459.
- Breitbach, Z. S., Berthod, A., Huang, K. & Armstrong, D. W., 2015. Mass spectrometric detection of trace anions: The evolution of paired-ion electrospray ionization (PIESI). *Mass Spectrometry Reviews*, 35(2), pp. 201-218.
- Cappiello, A. et al., 2008. Overcoming Matrix Effects in Liquid Chromatography–Mass Spectrometry. *Analytical Chemistry*, 80(23), pp. 9343-9348.
- Cha´vez-Santoscoy, R. A. et al., 2014. Conjugated and free sterols from black bean (*Phaseolus vulgaris* L.) seed coats as cholesterol micelle disruptors and their effect on lipid metabolism and cholesterol transport in rat primary hepatocytes. *Genes & Nutrition*, 9(1), pp. 367-376.
- Connors, K. A. & Pandit, N. K., 1978. N-Methylimidazole as a Catalyst for Analytical Acetylations of Hydroxy Compounds. *Analytical Chemistry*, 50(11), pp. 1542-1545.
- Coskun, O., 2016. Separation techniques: Chromatography. *Northern Clinics of Istanbul*, 3(2), pp. 156-160.
- DeJongh, D. C. et al., 1969. Analysis of Trimethylsilyl Derivatives of Carbohydrates by Gas Chromatography and Mass Spectrometry. *Journal of the American Chemical Society*, 91(7), pp. 1728-1740.
- Diesel, R., 1895. *METHOD OF AND APPARATUS FOR CONVERTING HEAT INTO WORK*. [Online] Available at: <https://patentimages.storage.googleapis.com/f8/f1/cf/35d927d0ad9638/US542846.pdf> [Accessed 5 March 2018].
- Eide, I. & Zahlsten, . K., 2007. Chemical Fingerprinting of Biodiesel Using Electrospray Mass Spectrometry and Chemometrics: Characterization, Discrimination, Identification, and Quantification in Petrodiesel. *Energy & Fuels*, 21(6), pp. 3702-3708.
- El-Aneed, A., Cohen, A. & Banoub, J., 2009. Mass Spectrometry, Review of the Basics: Electrospray, MALDI, and Commonly Used Mass Analyzers. *Applied Spectroscopy Reviews*, 44(3), pp. 210-230.

- Fenselau, C., 1992. TANDEM MASS SPECTROMETRY: The Competitive Edge for Pharmacology. *Annual Review of Pharmacology and Toxicology*, 32(1), pp. 555-578.
- Gerpen, J. V., He, B. B. & Duff, K., 2011. *Measurement and Control Strategies for Sterol Glucosides to Improve Biodiesel Quality – Year 2*, Idaho: National Institute for Advanced Transportation.
- Gui, M. M., Lee, K. T. & Bhatia, S., 2008. Feasibility of edible oil vs. non-edible oil vs. waste edible oil as biodiesel feedstock. *Energy*, 33(11), pp. 1646-1653.
- Guo, M., Song, W. & Buhain, J., 2015. Bioenergy and biofuels: History, status, and perspective. *Renewable and Sustainable Energy Reviews*, Volume 42, pp. 712-725.
- Gutiérrez, A. & del Río, J. C., 2001. Gas chromatography/mass spectrometry demonstration of steryl glycosides in eucalypt wood, Kraft pulp and process liquids. *Rapid Communications in Mass Spectrometry*, 15(24), pp. 2515-2520.
- Hassan, . M. H. & Abul Kalam, M., 2013. An overview of biofuel as a renewable energy source: development and challenges. *Procedia Engineering*, Volume 56, pp. 39-35.
- Ho, C. et al., 2003. Electrospray Ionisation Mass Spectrometry: Principles and Clinical Applications. *Clinical Biochemist Reviews*, 24(1), pp. 3-12.
- Hoed, V. V. et al., 2008. Identification and Occurrence of Steryl Glucosides in Palm and Soy Biodiesel. *Journal of the American Oil Chemists' Society*, 85(8), pp. 701-709.
- Josling, T., Blanford, D. & Earley, J., 2010. *Biofuel and Biomass Subsidies in the U.S., EU and Brazil: Towards a Transparent System of Notification*, s.l.: International Food & Agricultural Trade Policy Council.
- Kamel, A. M., Brown, P. R. & Munson, B., 1999. Effects of Mobile-Phase Additives, Solution pH, Ionization Constant, and Analyte Concentration on the Sensitivities and Electrospray Ionization Mass Spectra of Nucleoside Antiviral Agents. *Analytical Chemistry*, 72(24), pp. 5481-5492.
- Knights, B. A., 1973. Gas-Liquid Chromatography of Sterol Glycosides. *Analytical Letters*, 6(6), pp. 495-503.
- Knothe, G., 2001. Historical perspectives on vegetable oil-based diesel fuels. *Industrial Oils*, Volume 12, pp. 1103-1107.
- Koplow, D., Earth Track, Inc. Cambridge & MA, 2006. *Biofuels – At What Cost? Government support for ethanol and biodiesel in the United States*, Winnipeg: International Institute for Sustainable Development (IISD).
- Kovganko, N. K. & Kashkan, Z. N., 1999. STEROL GLYCOSIDES AND ACYLGLYCOSIDES. *Chemistry of Natural Compounds*, 35(5), pp. 479-497.
- Kutas, G., Lindberg, C. & Steenblik, R., 2007. *Biofuels: At What Cost? Government Support for Ethanol and Biodiesel in the European Union*, Winnipeg: International Institute for Sustainable Development (IISD).
- Laine, R. A. & Elbein, A. D., 1971. Steryl glucosides in *Phaseolus aureus*. Use of gas-liquid chromatography and mass spectrometry for structural identification. *Biochemistry*, 10(13), p. 2547–2553.

- Lascoste, F., Dejean, F., Griffon, H. & Rouquette, C., 2009. Quantification of free and esterified sterol glucosides in vegetable oils and biodiesel. *European Journal of Lipid Science and Technology*, 111(8), pp. 822-828.
- Lee, I. et al., 2007. *The Role of Sterol Glucosides on Filter Plugging*, Grand Forks: BBI International.
- Leitner, A., Emmert, J., Boerner, K. & Lindner, W., 2007. Influence of Solvent Additive Composition on Chromatographic Separation and Sodium Adduct Formation of Peptides in HPLC–ESI MS. *Chromatographia*, 65(11-12), pp. 649-653.
- Lepage, M., 1964. Isolation and characterization of an esterified form of sterol glucoside. *Journal of Lipid Research*, 5(4), pp. 587-592.
- Leung, D. Y., Wu, X. & Leung, M. K., 2010. A review on biodiesel production using catalyzed transesterification. *Applied Energy*, 87(4), pp. 1083-1095.
- Licea-Perez, H., Junnotula, V., Zohrabian, S. & Karlinsey, M., 2016. Development of multi-sugar LC-MS/MS assay using simple chemical derivatization with acetic anhydride. *Analytical Methods*, 8(15), pp. 3023-3033.
- Lopez, G. P. & Laan, T., 2008. *Biofuels — At What Cost? Government support for biodiesel in Malaysia*, Winnipeg: International Institute for Sustainable Development (IISD).
- Mateparae, J., 2011. *Engine Fuel Specification Regulations 2011 (S/R 2011/352)*, Wellington: New Zealand Government.
- Matreya LLC, 2018. *Sterol Glucosides*. [Online]
Available at: http://www.matreya.com/Products/Steryl-Glucosides_1117.aspx
[Accessed 18 April 2018].
- Mjøs, S. A., 2004. The prediction of fatty acid structure from selected ions in electron impact mass spectra of fatty acid methyl esters. *European Journal of Lipid Science and Technology*, 106(8), pp. 550-5560.
- Monirul, I. M. et al., 2015. A comprehensive review on biodiesel cold flow properties and oxidation stability along with their improvement processes. *Royal Society of Chemistry*, 5(105), pp. 86631-86655.
- Montpetit, A. & Tremblay, A. Y., 2016. A Quantitative Method of Analysis for Sterol Glycosides in Biodiesel and FAME Using GC-FID. *Journal of the American Oil Chemists' Society*, 93(4), pp. 479-487.
- Moreau, R. M., Scott, K. M. & Haas, M. J., 2008. The Identification and Quantification of Steryl Glucosides in Precipitates from Commercial Biodiesel. *Journal of the American Oil Chemists' Society*, 85(8), pp. 761-770.
- Peiru, S. et al., 2015. An industrial scale process for the enzymatic removal of sterol glucosides from biodiesel. *Biotechnology for Biofuels*, 8(223), pp. 1-12.
- Pfalzgraf, L., Lee, I., Foster, J. & Poppe, G., 2007. Effect of minor components in soy biodiesel on cloud point and filterability. *Biorenewable Resources*, Volume 4, pp. 17-21.
- Phillips, K. M., Ruggio, D. M. & Ashraf-Khorassani, M., 2005. ANALYSIS OF STERYL GLUCOSIDES IN FOODS AND DIETARY SUPPLEMENTS BY SOLID-PHASE EXTRACTION AND GAS CHROMATOGRAPHY. *Journal of Food Lipids*, 12(2), pp. 124-140.

- Rahman, M. et al., 2015. Basic Overview on Gas Chromatography Columns. In: J. Anderson, A. Berthod, V. Pino & A. Stalcup, eds. *Analytical Separation Science*. s.l.:Wiley-VCH Verlag GmbH & Co. KGaA, pp. 823-834.
- Reddy, P., 2017. *Engine Fuel Specifications Amendment Regulations 2017*, Wellington: Parliamentary Counsel Office.
- Schrack, K. et al., 2011. Steryl Glucoside and Acyl Steryl Glucoside Analysis of Arabidopsis Seeds by Electro spray Ionization Tandem Mass Spectrometry. *Lipids*, 47(7), pp. 185-193.
- Sigma-Aldrich, 2018. *Sigma-Aldrich*. [Online]
Available at: www.sigmaaldrich.com
[Accessed 8 April 2018].
- Siuzdak, G., 2004. An Introduction to Mass Spectrometry Ionization: An Excerpt from The Expanding Role of Mass Spectrometry in Biotechnology, 2nd ed.; MCC Press: San Diego, 2005. *SLAS TECHNOLOGY: Translating Life Sciences Innovation*, 9(2), pp. 50-63.
- Songtawee, S., Ratanawilai, S. & Tongurai, C., 2014. Effect of Sterol Glucosides in Biodiesel Production. *International Journal of Advances in Chemical Engineering and Biological Sciences (IJACEBS)*, 1(1), pp. 2349-1515.
- Tenenbaum, D. J., 2008. Food vs. Fuel: Diversion of Crops Could Cause More Hunger. *Environmental Health Perspectives*, 116(6), pp. A254-A257.
- Tiwari, P., Kumar, R., Maulik, P. R. & Misra, A. K., 2005. Efficient Acetylation of Carbohydrates Promoted by Imidazole. *European Journal of Organic Chemistry*, 2005(20), pp. 4265-4270.
- Tomei, J. & Helliwell, R., 2016. Food versus fuel? Going beyond biofuels. *Land Use Policy*, Volume 56, pp. 320-326.
- Wang, H., Tang, H., Salley, S. & Simon Ng, K. Y., 2009. Analysis of Sterol Glycosides in Biodiesel and Biodiesel Precipitates. *Journal of the American Oil Chemists' Society*, 87(2), pp. 215-221.
- Wewer, V., Dombrink, I., Dorp, K. v. & Dörmann, P., 2011. Quantification of sterol lipids in plants by quadrupole time-of-flight mass spectrometry. *Journal of Lipid Research*, 52(5), pp. 1039-1054.
- Yahaya, M. F. et al., 2013. A review on the Chromatographic Analysis of Biodiesel. *International Journal of Education and Research*, 1(8), pp. 1-12.
- Yasin, M. H. M. et al., 2013. Fuel Physical Characteristics of Biodiesel Blend Fuels with Alcohol as Additives. *Procedia Engineering*, Volume 53, pp. 701-706.